Active eukaryotes in microbialites from Highborne Cay, Bahamas and Hamelin Pool (Shark Bay), Australia

Edgcomb, Virginia P.[1*], Joan M. Bernhard[1], Roger E. Summons[2], William Orsi[1], David Beaudoin[1], Pieter T. Visscher[3]

[1]Department of Geology and Geophysics, Woods Hole Oceanographic Institution, Woods Hole, Massachusetts, USA
[2]EAPS Department, Massachusetts Institute of Technology, Boston, Massachusetts, USA
[3]Department of Marine Sciences, University of Connecticut, Groton Connecticut, USA

*Corresponding Author: Virginia P. Edgcomb. Tel.: 508-289-3734, email: vedgcomb@whoi.edu

Keywords: eukaryote, protist, stromatolite, microbialite, thrombolite, 18S rRNA, diversity, foraminifera, Hamelin Pool, Highborne Cay

ABSTRACT

Microbialites are organosedimentary structures that are formed through the interaction of benthic microbial communities and sediments and include mineral precipitation. These lithifying microbial mat structures include stromatolites and thrombolites. Exuma Sound in the Bahamas, and Hamelin Pool in Shark Bay, Western Australia are two locations where significant stands of modern microbialites exist. Although prokaryotic diversity in these structures is reasonably well documented, little is known about the eukaryotic component of these communities and their potential to influence sedimentary fabrics through grazing, binding and burrowing activities. Accordingly, comparisons of eukaryotic communities in modern stromatolitic and thrombolytic mats can potentially provide insight into the coexistence of both laminated and clotted mat structures in close proximity to one another. Here we examine this possibility by comparing eukaryotic diversity based on Sanger and high-throughput pyrosequencing of small subunit ribosomal RNA (18S rRNA) genes. Analyses were based on total RNA extracts as template to minimize input from inactive or deceased organisms. Results identified diverse eukaryotic communities particularly stramenopiles, Alveolata, Metazoa, Amoebozoa, and Rhizaria within different mat types at both locations, as well as abundant and diverse signatures of eukaryotes with <80% sequence similarity to sequences in GenBank. This suggests presence of significant novel eukaryotic diversity, particularly in hypersaline Hamelin Pool. There was evidence of vertical structuring of protist populations and foraminiferal diversity was highest in bioturbated/clotted thrombolite mats of Highborne Cay.

INTRODUCTION

Fossilized stromatolites, dating back to 3.45 billion years ago, comprise the earliest visible record of life on Earth (e.g. Allwood *et al*., 2006; Grotzinger and Knoll, 1999; Walter, 1983). There are only a few locations in the world where modern analogues of marine stromatolites are actively forming, and these include the margin of Exuma Sound,

with regular seawater salinity, Bahamas (Reid *et al*. 2000), and hypersaline Hamelin Pool, Australia (Jahnert and Collins, 2011). Stromatolites are laminated microbialites, that can be further classified according to degree of lithification and cell-taxonomic richness of different microbial groups (discussed in Baumgartner *et al*. 2009; Foster *et al*. 2009). Hamelin Pool and Exuma Sound are both sites of formation of oolitic sands and lithifying microbial mats. Additional carbonate occurs in these environments, including in the form of metazoan skeletal remains and micrite. These carbonates are trapped and bound by extracellular polymeric substances (EPS), produced by filamentous cyanobacteria and other bacteria (Dupraz and Visscher, 2005; Reid et al. 2000). Thrombolites are microbialites that lack lamination, having instead, a clotted fabric. Some attribute this to a specific microbial flora and contend thrombolites are essentially a lower Paleozoic phenomenon (Kennard and James, 1986). Others propose thrombolites result from 'remodeling of a precursor fabric' by a combination of processes that include physical and metazoan disruption (Planavsky and Ginsburg, 2009; Walter and Heys, 1985). Regardless, both types of microbialites reflect the activities of complex microbial communities and their interactions with the environment. A better understanding of factors influencing microbialite structure has implications for interpretation of the paleorecord.

While stromatolites are characterized by steep gradients of oxygen, sulfide and light (Visscher and Stolz, 2005; Visscher *et al*. 1998; summarized in Dupraz *et al*. 2009), thrombolites often lack a single oxygen maximum and the oxic zone typically extends to greater depth (Myshrall *et al.* 2010). Independent of the debate on the origins of thrombolites, it seems likely grazing, burrowing, and sediment-binding activities of specific eukaryotes such as the foraminifera may significantly contribute to the more bioturbated mat structures (Bernhard *et al*. 2013). In alternative proposals, thrombolites might result from interactions between eukaryotic green algae and various coralline algae (Feldmann & McKenzie, 1998), the patchy calcification of the filamentous cyanobacterium *Dichotrix* (Planavsky *et al.* 2009), or by a combination of coccoid and filamentous cyanobacterial photosynthesis, as was proposed for Green Lake, Fayetteville, NY, USA (Thompson *et al*., 1990).

Flagellate protists have been identified in some modern stromatolites (Al-Qassab *et al.*, 2002), as well as ciliates in stromatolite microbial nodules (Westphalen, 1993), and foraminiferal tests (shells) in some thrombolites (e.g., Mastandrea *et al.*, 2006; Papineau *et al.*, 2005). These three groups are known to be successful in sulfide-enriched, oxygen-depleted environments (e.g., Bernhard, 2003; Bernhard *et al.*, 2006; Fenchel and Finlay, 1995). Myshrall *et al.* (2010) propose a relatively minor role for eukaryotes in thrombolites, and suggest based on the lower diversity and higher productivity they detected in thrombolites compared to stromatolites, that thrombolite communities are distinct from those in adjacent stromatolites, and not simply 'bioturbated stromatolites.'

Due to the limited depth of sequencing and methodological biases (e.g., primer choice), numerous other potentially bioturbating eukaryotes may have been undetected by Myshrall *et al.* (2010). Here, we analyzed eukaryotic communities in different microbialite structures along the margin of Exuma Sound, Bahamas, and in Hamelin Pool, Australia by applying high-throughput sequencing of eukaryotic SSU rRNA combined with multivariate statistical analyses. By utilizing RNA and not DNA as template, we focus on the active fraction of the community in order to determine: a) if the eukaryotic composition in different microbialite types is distinct, b) if there are common communities in microbialites at both locations, and c) if a greater diversity of SSU rRNA signatures of potential eukaryotic bioturbators other than metazoa can be found in more clotted microbialites that might help explain their structure.

MATERIALS AND METHODS

Field site and sample collection

Samples of microbialite mat types were collected from just below the water line at low tide on the windward side of Highborne Cay (24°43.5'N, 76°49'W), Bahamas in March 2010 and from Hamelin Pool near Carbla Station on Hamelin Pool, Australia (26°15.4'S, 114°13.5'E) in June 2011. Highborne microbialite mat types were designated according to Reid *et al*. (2000) for stromatolite (i.e., laminated) mats and according to Myshrall *et al.* (2010) for thrombolite (i.e., clotted) mats. Samples collected at Highborne included stromatolite surface Type 1 mats, which result from binding and trapping of ooids by the filamentous cyanobacterium *Schizothrix* sp., surface Type 2 mats, which are biofilm

structures comprised of a complex community that includes aerobic and anaerobic heterotrophic prokaryotes that precipitate a microcrystalline (ca. 30 μm in diameter) $CaCO_3$ crust, Incipient Type 2 mats (transitioning from Type 1 to Type 2, with crust firming, but not complete), and thrombolitic mats, referred to as button types by Myshrall *et al*. (2010), which are irregular, clotted structures.

Hamelin Pool microbialites, which were classified using nomenclature of Jahnert and Collins (2011) and Logan (1961), included pustular mats, which are irregular, clotted mats, colloform mats, which are coarse, laminoid wavy mats, and smooth mats, which are fine, laminoid structures. In Hamelin Pool we also sampled a smooth mat that was recently scoured ("smooth scoured"). Only the 1-2cm fraction of this was sampled because of disturbance to the top 1 cm. We also sampled the water column (500 ml) in the immediate vicinity of these microbialite types, as well as sulfidic waters (~2m below pool surface) of a nearby 'blue hole' (a stratified shallow hypersaline [78 PSU] pool on a platform on the western edge of Hamelin Pool ~20 km from the microbialite sampling site) for comparison. Samples from both locations are described in Table 1. The salinity at the time of collection was 33-35.5 PSU at Highborne, and 66-72 PSU at Hamelin Pool. Water temperature at Highborne during sampling was 25.4-25.9°C and in Hamelin Pool, 14.1-15.0°C. Maximum light intensity during midday at Highborne and Hamelin Pool during the time of sampling was between 2000-2100 $\mu Em^{-2}s^{-1}$ and 1100 and 1300 $\mu Em^{-2}s^{-1}$, respectively. Microbialite samples were collected using 50cc syringe cores (2.6-cm inner diameter), which were immediately sectioned into 1-cm intervals to 2 cm and preserved in RNALater (Ambion).

Microelectrode measurements

Depth profiles of oxygen, sulfide and pH were determined using needle microelectrodes (Visscher *et al*. 1998, 2002, Myshrall *et al.* 2010) *ex situ* under ambient temperature and light intensity. Small samples (~5x5 cm) were collected and submerged in 3 cm water collected from the site and pre-incubated for 12-24hr prior to the first measurement. Daytime electrode readings were carried out during the peak of photosynthesis between noon and 2pm, and nighttime measurements were made at the end of the dark period between 3:30 and 5:30am. Light measurements were done using a LiCor LI 250 meter

equipped with a SA190A quantum sensor and salinity and temperature measurements were obtained with an Accumet AP75 temperature/conductivity meter.

RNA extraction and small subunit ribosomal RNA (SSU rRNA) gene sequencing

Samples stored in RNAlater (0.5 gm of preserved material) were rinsed three times with RNAse-free and sterile 1X phosphate buffered saline (PBS) prior to RNA extraction. RNA was extracted using the FastRNA Pro Soil-Direct Kit (MP Biomedical). The manufacturer's extraction protocol was modified to include the addition of 2M sodium acetate following cell lysis and a Turbo DNase (Ambion) treatment prior to the RNA Matrix cleanup included in the extraction kit. DNA removal was confirmed by 45 cycles of PCR (see below) using extracted RNA as template. RNA was reverse transcribed and PCR amplified in one step using the Superscript One-Step RT-PCR kit (Invitrogen) and either general eukaryotic small subunit ribosomal RNA (SSU rRNA) gene V4 hypervariable region primers and protocols (TAReuk454FWD1/ TAReukREV3, Stoeck *et al.* 2010) or general primers for foraminifera (S14F1/S17, Pawlowski 2000). The foraminifera-specific amplifications were required because general V4 primers do not detect most foraminifera. Barcoded PCR products were purified from 1% agarose gels using the Zymoclean Gel DNA Recovery Kit (Zymo Research). Foraminiferal PCR products were cloned into pCR4-TOPO using the TOPO TA Cloning Kit (Invitrogen) for Sanger sequencing (1 96-well plate per microbialite sample).

Pyrotags and clone sequences were processed for quality control and chimera removal using Bellerophon Chimera Check and the Check_Chimera utilities (Ribosomal Database Project) (Cole *et al.* 2003). After denoising of the pyrosequencing dataset using AmpliconNoise (Quince *et al.* 2009), sequences from clone libraries and pyrosequencing were clustered into operational taxonomic units (OTUs) at 97% similarity in QIIME (Caporaso et al. 2010), and taxonomy of OTU representatives was assigned using JAguc (Nebel *et al*. 2011). Taxonomy was linked to the QIIME OTU table via a PERL script available from the authors. Since V4 primers did not encompass foraminifera, the V4 and clone library datasets were clustered separately and then 97% OTUs were combined from each library for each sample. We ran ordination and statistical analyses (described in detail below) on both foraminifera-only, and combined datasets. For combined datasets,

we ran analyses using non-normalized data sets as well as normalized datasets, where V4 libraries were resampled to generate data sets of similar size to our foraminiferal data sets. Normalization did not produce a different outcome, and so to retain the most detailed picture of eukaryotic diversity, we present the non-normalized analyses. An unweighted presentation of diversity data (stacked histograms) in each sample was used for foraminifera-only analyses, since clone libraries may not be saturated. Weighted analyses were used for total eukaryotes (combined foraminiferal clone and pyrosequencing data). We interpret fine scale taxonomic assignments (species-level; sometimes genus-level assignments) with caution because BLAST-based assignments are complicated by the hypervariable nature of the V4 region of eukaryotic rRNA. Variable taxon representation in public databases means JAguc may make taxonomic assignments down to genus or species, but in others, only down to higher levels. Accordingly, our stacked histograms presenting snapshots of diversity typically do not present a single level of taxonomic resolution.

The BLASTn output and the OTU table were combined to calculate the number of sequences across each sample belonging to a specific taxonomic group. The relative abundance of each protistan group in a given sample was calculated as a percentage value by dividing the raw number of sequences associated with the specific taxon by the total number of sequences in the sample. This was used to generate heatmaps in QIIME.

Cannonical correspondence analysis (CCA) was used to visualize relationships between community structure and concentrations of dissolved oxygen, sediment depth, and sites. Multi-Response Permutation Procedure (MRPP) was used as a statistical test of significance for each of these factors on OTU distribution. A Monte Carlo test was also used to assess a null hypothesis of no relationship between OTU distribution and these variables. Ordination and multivariate statistics were performed on our dataset clustered at 97% sequence identity threshold. MRPP, Monte Carlo tests, and CCA analyses used the PC-ORD software package (MjM Software Design, Gleneden Beach, OR, USA). Non-metric multidimensional scaling (NMS; goodness of fit measured by stress values, with values <15 indicating a low probability of drawing the wrong inferences from the results) and Principal Component Analysis, as implemented within PC-ORD, were used to confirm CCA results (data not shown). An unweighted Unifrac analysis comparing the

eukaryotic communities (beta diversity) in all Hamelin Pool and Highborne Cay samples was performed within QIIME.

Nucleotide sequences for foraminifera have been deposited in GenBank (Accession numbers JX872558 - JX873273 (Hamelin Pool) and JX873274 - JX873955 (Highborne Cay)). V4 pyrosequencing tag sequences for Highborne Cay and Hamelin Pool have been deposited in the GenBank (SRA061992 and SRA061825, respectively).

RESULTS

After removal of low-quality and potentially chimeric sequences, pyrosequencing yielded a total of ~150,000 eukaryotic tags and Sanger sequencing produced 733 and 820 foraminifera clone sequences for Hamelin Pool and Highborne, respectively. The Hamelin Pool and Highborne datasets were clustered into 2388 (including 129 foraminiferal) and 1571 (including 96 foraminiferal) OTUs, respectively. These data were interpreted together with physicochemical data (Table 1).

Eukaryotic SSU rRNA diversity in Highborne Cay, Bahamas microbialites

All mat types appear to support diverse eukaryotes, however significant differences in SSU rRNA signatures are not generally observed between different mat types above Order-level. Groups with the greatest representation in combined Sanger and pyrosequencing libraries were (in decreasing order): stramenopiles (e.g. diatoms), Alveolata (ciliates and dinoflagellates), Metazoa (Annelids, Cnidaria, Gastrotricha, Nematoda, Platyhelminthes, and Echinodermata), Amoebozoa, and Rhizaria (Figure 1). However, within those dominant groups, there were differences in composition between mat types and between depths. For example, within Rhizaria (which includes foraminifera), Type 1 mat signatures in the 0-1cm fraction affiliated with the foraminiferal taxa Texulariida, Miliolina, 3 types of Rotaliida, and undescribed foraminifers with no close described relatives in GenBank (80% sequence similarity cutoff) (Figure 2). In the 1-2 cm fractions, signatures of Allogromida were detected. Replicate 0-1cm samples from two Incipient Type 2 mats were different in composition and relative proportions of foraminiferal OTUs, and different in composition from Type 1

mats, with more than half of OTUs coming from Textulariida (Figure 2). Differences may represent variations in the transitional state of one mat type to another. Thrombolite samples had the highest foraminiferal diversity; sixteen OTUs in the 0-1cm fraction, and 14 OTUs in the 1-2cm fraction (Figure 2), and differences between the 0-1 and 1-2 cm fractions. A heatmap of foraminiferal OTUs indicates unique foraminiferal populations inhabiting thrombolites compared to stromatolites (Figure 3). Ciliate OTUs represented >50% of alveolate OTUs (Figure 1), with no clear difference in community composition between mat types and representatives from almost every ciliate class (10/12) (Supplementary Figure 1).

CCA of the Highborne data indicates that mat type and depth below the sediment-water interface explain much of the observed community structure (30% of the variation explained by axes 1 and 2 together). Values for MRPP tests of significance were combined for sediment depth and oxygen for all data sets because all 0-1cm samples were at least partly oxic and all 1-2cm samples were anoxic. The analysis shows a separation of protist communities within samples from different mat types and between the 0-1 and 1-2cm fractions (Figure 4). CCA analysis considering depth and mat type also explains 31% of the foraminifera sequence variation, and shows a clear separation between the 0-1 cm fraction and the 1-2 cm fractions (Figure 5). Depth/oxygen was found to have a significant effect ($p \leq 0.05$) on foraminifera OTU distributions in Highborne samples, and mat type was found to have a significant effect on whole eukaryotic community OTU distribution (Table 2).

Eukaryotic SSU rRNA gene diversity in Hamelin Pool, Australia microbialites

Eukaryotic rRNA sequences were dominated by Alveolata (10-50%), stramenopiles (10-30%), and unclassified eukaryotes (5-45%) (Figure 6). Alveolates were dominated by Heterocapsaceae and *Protodinium* (Dinophyceae) in colloform mats (with more diversity of alveolates in the 1-2cm fraction), and Litostomatea (Ciliophora) in smooth mats. Pustular mats had the greatest variety of ciliate and dinoflagellate OTUs, most of which were also represented in the overlying water-column sample (Supplementary Figure 2).

The Hamelin Pool (Carbla Beach) water sample collected from above the microbialites had almost 40% of total OTUs from fungi, 35% from stramenopiles, and

signatures of metazoa, choanoflagellates, rhizarians, glaucocystophytes (primarily a freshwater algae group), and low (<5%) contribution from unclassified eukaryotes. OTUs present in the sulfidic water sample from the shallow hypersaline 'blue hole' at a distant location on the western shore of Hamelin Pool, were distinct from those in Hamelin Pool, likely due to presence/absence of sulfide.

Stramenopile OTUs were distinct between the local water samples and the microbialite samples (Supplementary Figure 3). The water samples were dominated by diatom stramenopiles, and microbialite stramenopiles were dominated by labyrinthulids. Between the two water samples, stramenopile OTUs in the sulfidic 'blue hole' (90% Bacillariophyceae) were distinct from those in the sulfide-free seawater at Carbla Station (50% Coscinodiscophyceae and ~40% silicoflagellates affiliating with Dictyochophyceae). Labyrinthulids affiliating to Thraustrochytridae represented between 60 and 85% of microbialite stramenopile sequences. Ten to fifty percent of OTUs were unassigned (defined as having <80% similarity to GenBank sequences) suggesting the presence of a novel eukaryotic community in Hamelin Pool, which will be the subject of a future study.

Smooth mats were dominated by Alveolata (50-90% ciliates), stramenopiles (~20%), and unclassified eukaryotes (10-20%) (Figure 6). Dinoflagellate representatives in the 0-1 cm fraction included 40% Gymnodiniales, and several other taxa. In the 1-2 cm fraction, 90% of alveolate OTUs affiliated with Litostomatea (Ciliophora). The smooth mat that had been recently scoured (sample "SS") exhibited a shift in eukaryotic composition.

The colloform mats differed from the smooth mats by having a slightly lower contribution from alveolate signatures, and shifts within the alveolate signatures (Supplementary Figure 2), with OTUs affiliating with Dinophyceae dominating at both depth intervals. The pustular mat sample (only the 0-1cm fraction was analyzed) differed from the others by having a greater representation of rhizarian signatures, new contributions from Cryptophyta, and no signatures from Centroheliozoa.

When examining foraminiferal sequences from Hamelin Pool microbialites, differences in community composition are observed between microbialite types and between depths within a single mat core (Figure 7). Smooth mat samples were dominated

by one OTU within Rotaliida. In the 0-1cm fraction, there were additional OTU contributions from Textulariida, Rotaliida, Milliolina, and Allogromida (i.e., thecate, or non-mineralized forms). Relative to the unscoured smooth mat, the scoured smooth mat had 8 vs. 2 OTUs at the 1-2 cm depth, and mostly distinct OTUs, overall.

Foraminiferal OTU compositions in the two depth fractions of the colloform and smooth mats were very different from one another (3 out of 8, and 3 out of 13 overlapped, respectively) (Supplementary Figure 4). The pustular mat type exhibited a distinct foraminiferal community composition in the 0-1 cm fraction, with 85% of the OTUs coming from Miliolina, and the rest from Allogromida (Supplementary Figure 4). A heatmap of foraminiferal OTUs supports the unique nature of foraminiferal communities in the different mat types (minimal overlap) and depth intervals within individual microbialite types (Supplementary Figure 5).

CCA of our Hamelin Pool microbialite data identified mat type and depth as parameters that impact much of the observed protistan community distribution. This analysis supports the differentiation of eukaryote communities within different microbialite types and between different depths within individual microbialite types (Figure 7). As observed in our Highborne data, depth/oxygen was found to have a significant effect ($p \leq 0.05$) on the observed distribution of OTUs for the foraminiferal data set only. Significantly different eukaryotic communities inhabit different mat types.

Combined CCA analysis of eukaryotic SSU rRNA diversity

Highborne and Hamelin Pool each contain distinct eukaryote communities (including foraminifera). Microbialite type and depth explained only 22.8% of the variation in a combined CCA analysis, implying other environmental factors such as salinity are driving most of the community differences between these two sites (Supplementary Figure 6). This notion is supported by MRPP analysis of this combined data set, where salinity is shown to be a significant influence ($p \leq 0.05$) on eukaryotic OTU composition (Table 2). Site had a significant impact on distribution of OTUs for foraminifera separately. For the inclusive eukaryotic data set, mat type and site had a significant effect on distribution of OTUs.

DISCUSSION

A new view of eukaryotic microbial diversity in microbialites. Microbialites in Hamelin Pool and Highborne Cay have been the subject of several recent investigations into their microbial communities and biogeochemistry (e.g., Baumgartner *et al*. 2009; Myshrall *et al.* 2010; Visscher *et al*. 1998; Reid *et al*. 2000; Foster *et al*. 2009; Foster and Green 2011; Allen *et al.* 2009; Burns *et al.* 2004). To our knowledge, only three studies have gathered information on microbial eukaryotes, one for Hamelin Pool (Allen *et al.* 2009) and two for Highborne (Baumgartner *et al.* 2009; Myshrall *et al.* 2011); and in comparison to this study, were more limited (and DNA-based) rRNA gene sequencing efforts. In the study of Hamelin Pool microbialites, only a limited number of signatures (11 unique clones from a pustular mat sample, and 10 from a smooth mat) were detected, and most were from Nematodes (Allen *et al.* 2009). Fungal, tardigrade, and microalgal OTUs were also detected. When using small sediment volumes and clone libraries, libraries can often be saturated by metazoan sequences. This was observed previously in microbialite samples, where nematode sequences dominated eukaryotic sequences in marine (Baumgartner *et al.* 2009; Feazel et al. 2008) and in freshwater microbialites (Couradeau *et al.* 2011).

In one of the studies of Highborne thrombolites, Myshrall *et al.* (2010) recovered low eukaryote diversity (only 26 unique eukaryotic ecotypes) relative to bacteria, with nematode sequences again figuring prominently in their clone libraries. Myshrall *et al.* (2010) also detected members of Alveolata and Chlorophyta, including sequences affiliating with those from hypersaline mats of Guerrero Negro (Feazel *et al*. 2008) and sequences in public databases from Hawaii Volcanoes National Park (HAVO) cave mats. They attributed their low recovered eukaryotic diversity in Highborne thrombolites at least in part, to the dynamic nature of microbialite environments, where they are periodically buried in oolitic sands, potentially for months (e.g. Reid *et al.* 2000). PCR primers can also influence recovered diversity. While no PCR primer set can be assumed to be inclusive for its target group, in the original description of the primers used by Myshrall *et al*. (Moon-van der Staay *et al.* 2001), it is acknowledged this set has biases against certain groups of eukaryotes including Chrysophyceae, some Chlorarachniophyceae, some Apicomplexa, some Ciliophora, and deep-branching

372 eukaryotes. In addition, we have found this set to be biased against many members of
373 foraminifera, precluding its use in this study. The inclusion of foraminifera and other
374 groups such as Ciliophora is particularly important for making valid comparisons of
375 different microbialite communities.
376 Our analysis reveals diverse communities of eukaryotes in all microbialite types
377 at both sites. The major difference in results (high vs. low diversity) can be attributed to
378 different nucleic acid extraction procedures, templates (RNA vs. DNA), PCR primers,
379 and sequencing efforts/technologies. We attempted to minimize methodological biases by
380 combining pyrosequencing of the V4 region of the SSU rRNA with Sanger clone
381 libraries specifically targeting the foraminifera (missed by the employed V4 primers). In
382 spite of the greater depth of sequencing in this study, for reasons explained above, and
383 because of minimal replication for specific microbialite types, we focus our observations
384 on broad differences in taxonomic composition of higher groups (family and higher)
385 between microbialite types that are likely representative of shifts in *in situ* populations.
386 CCA indicates distinct eukaryotic communities in the different microbialite types
387 and in different depth horizons within individual microbialite types in Highborne Cay and
388 Hamelin Pool (Figures 4 and 8). It is notable that the water samples analyzed from
389 Hamelin Pool (at the microbialite sampling site) and from the sulfidic 'blue hole' (away
390 from the sampling site) had eukaryotic communities largely distinct from the microbialite
391 samples (Figure 6 and Supplementary Figure 2). The sulfidic 'blue hole' water sample
392 also contained stramenopile species that were distinct from those in the Hamelin Pool
393 water sample, and dominated almost exclusively by diatoms, which are known to tolerate
394 sulfide (e.g. Nagai and Imai, 1999; Admiral and Pelletier 1979). In contrast, stramenopile
395 signatures from Hamelin Pool microbialites came primarily from Labyrinthulomycetes,
396 which are known to degrade complex polysaccharides (Raghukumar 2002). These
397 organisms may be attracted to, and involved in, the degradation of the abundant
398 polysaccharides in microbialite exopolymer matrices at this site.
399 The eukaryotic taxa that we report in microbialites at these two locations reflect
400 modern microbialite ecoystems in our present oxic biosphere. The extent that taxonomic
401 groups overlap with those in ancient microbialite ecoystems is unknown, primarily

because of their poor fossilization potential. Exploration of preserved eukaryotic biosignatures in fossilized microbialites is an area of future investigation.

Potential metazoan bioturbators. Stable isotope data indicate that filaments of the cyanobacterium *Dichotrix* play a role in formation of microbialite clots (Planavsky *et al.* 2009). Bioturbation by eukaryotes may also impact mat structures (Farmer 1992), and includes churning of sediments caused by movements of fauna. Many eukaryotes, including metazoa (e.g. Reichardt 1988; Pike *et al.* 2001), foraminifera (Gross, 2002), and ciliates (e.g. Glud and Fenchel 1999) are known to bioturbate sediments. Such activities stimulate bacterial community activity (Reichardt, 1988) and have been proposed as an explanation for the formation and coexistence of clotted mat structures such as thrombolites in the same vicinity as laminated mat structures (e.g. Type 1, 2, smooth and colloform mats) (Walter and Heys, 1985).

On Highborne Cay the dominant cyanobacteria in stromatolites (Type 1 and 2 mats) is *Schizothrix* (Reid *et al.* 2000) and in thrombolites is *Dichothrix* sp. (Myshrall *et al.* 2010; Planavsky *et al.* 2009). Previous studies have shown that nematodes may be attracted to volatile compounds produced by cyanobacteria via chemotaxis (Höckelmann *et al*. 2004). At Hamelin Pool, we detected signatures of diverse metazoa (Annelida, Cnidaria, Gastrotricha, Nematoda, Platyhelminthes, and Echinodermata), including specific nematode signatures detected previously (Allen *et al.*, 2009). Nematode signatures detected previously by Myshrall *et al.* (2011) and affiliating with *Syringolaimus* were found in Highborne microbialites.

Potential protist bioturbators. Bioturbation may occur as a result of feeding activities of ciliates and foraminifera (e.g. Pusch *et al.* 1998; Gross 2002) and biofilm degradation (e.g., by Thraustochytrids (Labyrinthulomycetes); Raghukumar 2002). Ciliate signatures figured prominently among alveolate OTUs in microbialites at both locations (Supplementary Figure 1). Alveolates in Hamelin Pool microbialites were dominated by dinoflagellate subgroups Heterocapsaceae and *Protodinium* in colloform mats, and by the ciliate class Litostomatea (includes taxa described from anoxic environments; Vd'ačny *et al*. 2011) in smooth mats. The 0-1cm and 1-2cm fractions of microbialite samples

contained very different alveolate communities that correlated with oxygen concentration (Table 1 and Supplementary Figure 3).

As noted above, foraminifera are also capable of significantly altering sediment fabric (e.g. Gross, 2002). The subgroup Allogromida feed on bacteria and smaller eukaryotes, are known to rend bacterial biofilms (Bernhard and Bowser, 1992), and through their reticulopodial activities can disrupt the fine laminations of microbialites (Bernhard *et al.*, 2013). Aside from some overlapping taxonomic groups, foraminiferal communities in different microbialite structures were distinct, and thrombolites harbored a greater family-level diversity than stromatolite types examined from Highborne (14-16 vs. 4-11) (Figure 2). Signatures affiliating with Allogromida were detected in the 1-2cm fraction of Type 1 stromatolite mats, and the 0-1cm fraction of Type 2 stromatolite as well as thrombolite mats from Highborne Cay, and the 0-1cm fraction of smooth, colloform, and pustular mats, and the 1-2cm fraction of colloform mats from Hamelin Pool (Supplementary Figure 4). No signatures of Allogromida were recovered from the 1-2cm fraction of smooth mat samples, consistent with their greater lamination. Heatmaps of foraminifera OTU distribution show very little taxonomic overlap between foraminiferal communities from either site (Figure 3 and Supplementary Figure 5). The distinction of foraminiferal communities between different depth fractions within the same mat type was supported by CCA and MRPP analyses for both Highborne and Hamelin Pool samples (Figures 5 and 8 and Table 2). Since foraminiferal populations can be patchy, the 0.5g samples processed for molecular analyses may under-sample foraminifera (and possibly other eukaryotic groups). Our study also did not examine whether or not there was a seasonal component, so it is possible that there are seasonal differences in protist communities at both of these sites, particularly Hamelin Pool, where relatively greater seasonal fluctuations in temperature, salinity, and light occur.

Comparison of Hamelin Pool and Highborne Cay eukaryotic communities. Unifrac Analysis shows a clear distinction between communities at each site (Figure 8). Differences are likely impacted by salinity and temperature. Hamelin Pool is a hypersaline system within the wider Shark Bay environment, with salinities between 66 and 72 PSU compared to 33-33.5 PSU at Highborne Cay, and had lower temperatures at

the time of sampling (14-15°C vs. 25.4-25.9°C) (Table 1). MRPP analyses of depth/oxygen, mat type, and salinity indicate that salinity drives, in part, the structure of the eukaryotic community ($p < 0.001$). It was impossible to differentiate between influences of depth and oxygen at the scale of our sectioning since all 1-2cm fractions were anoxic, and all 0-1cm fractions were at least partly oxic. Eukaryotic communities are distinct between microbialite types, and foraminiferal communities are distinct at different depths (Table 2), most likely the result of different types of habitat/substrate, and varying prokaryotic and algal populations. The observation that sediment depth is a more significant driver of foraminifera OTU composition than mat type in the combined analysis likely reflects sensitivity of different foraminiferal taxa to oxygen concentration and differences in ability to migrate in response to fluctuations in oxygen and sulfide occurring within microbialites during diurnal cycles. A similar pattern probably exists for other individual protistan taxonomic groups.

CONCLUSIONS

The sites sampled in this study are dynamic environments impacted by tides, storms, and currents, all of which subject microbialites to a continual cycle of mat construction and deconstruction. Eukaryotes in the different microbialite types at Highborne and Hamelin Pool were more diverse than previously reported, and distinct, suggesting they may shape or be shaped by different microbialite fabrics. Metazoa and protists are potential bioturbators of microbialite mat structure. Our analyses resulted in several hypotheses regarding the impact of eukaryotes on microbialite structures, including 1) eukaryotic bioturbation may contribute to the more clotted structures of several microbialite types, 2) eukaryotic communities transition in composition during mat rebuilding after scouring events, and as microbialites transition from one type to another, and 3) Protists such as Thraustochytrids may actively degrade/consume the mat extracellular matrix. These hypotheses can be tested using more refined sampling, time-course studies, laboratory-based experiments, and comparisons with non-lithifying, soft, organic-rich mats.

ACKNOWLEDGMENTS

We thank the captain and crew of the R/V *Walton Smith*, as well as the owners/operators of Carbla Station; World Heritage Site Ranger Ross Mack; Sabine Mehay, Sara Dilegge, Richard Sperduto, Anna McIntyre-Wressnig, Marti Jeglinski, and Ricardo Jahnert for field assistance; Philip Forte for assistance transporting field samples, and Kliti Grice and Anais Pages for laboratory support in Australia. We thank Jan Pawlowski and Andrea Habura for helpful discussions about PCR primers for foraminifera. We also thank two anonymous reviewers for comments on an earlier draft. This work was funded by grant OCE-0926421 to JMB and VPE and OCE-0926372 to RES.

Supplementary Information accompanies this paper on The ISME Journal website. The authors do not have any conflicts of interest to report regarding this manuscript.

TABLE AND FIGURE LEGENDS

Table 1. Temperature, Salinity, Oxygen, Sulfide, Temperature and Salinity data for Hamelin Pool, Australia and Highborne Cay, Bahamas microbialite samples. n/a = not observed. For sulfide data, depth noted is where free sulfide ($H_2S/HS^-/S^{2-}$) is first observed, and the maximum concentration during the day during sampling is based on single profiles (note: replicate profiles are very similar). Oxygen data are presented as the ranges of maximum depth and maximum % oxygen saturation in each sample.

Table 2. Multi Response Permutation Procedure (MRPP) P values for sample parameters for Highborne Cay (HC), Hamelin Pool (HP) and combined data sets. MRPP values are combined for depth and oxygen for all data sets because all 0-1cm samples were oxic and all 1-2cm samples were anoxic. na=not applicable.

Figure 1. Stacked histogram of eukaryotic OTU composition of (97% sequence similarity, weighted data presentation) in Highborne Cay, Bahamas microbialite samples

based on SSU rRNA signatures (cDNA template). Y-axis corresponds to fraction of OTUs affiliating with each taxonomic grouping out of 100%.

Figure 2. Stacked histogram of foraminiferal OTU composition of (97% sequence similarity, unweighted data presentation) in Highborne Cay, Bahamas microbialite samples based based on SSU rRNA signatures (cDNA template). Y-axis corresponds to fraction of OTUs affiliating with each taxonomic grouping out of 100%. Mat type noted for each sample (note: Type 1-2=Incipient Type 2 mat, Throm=Thrombolite).

Figure 3. Heatmap of foraminiferal OTUs (97% sequence similarity) from Highborne Cay, Bahamas. Y axis represents log transformed abundance. Mat type noted for each sample (note: Type 1-2=Incipient Type 2 mat, Throm=Thrombolite). Depths of fractions for each sample given in cm.

Figure 4. Biplot generated from Cannonical Correspondence Analysis (CCA) of the 18S rRNA data set from Highborne Cay, Bahamas, for all eukaryotes clustered at the 97% sequence identity level. Sampled microbialite types are circled. Depths of each sample are noted. Filled circles represent 0-1cm fractions, and hollow circles represent 1-2 cm fractions. Mat type noted for each sample (note: Type 1-2=Incipient Type 2 mat, Throm=Thrombolite).

Figure 5. Biplot generated from Cannonical Correspondence Analysis (CCA) of our 18S rRNA data set from Highborne Cay, Bahamas, for foraminiferal sequences clustered at the 97% sequence identity level. Line separates samples from 0-1 cm depths for different microbialite types. Depths of each sample are noted. Filled circles represent 0-1cm fractions, and hollow circles represent 1-2 cm fractions. Mat type noted for each sample (note: Type 1-2=Incipient Type 2 mat, Throm=Thrombolite).

Figure 6. Stacked histogram of eukaryotic OTU composition of (97% sequence similarity, weighted data presentation) in Hamelin Pool, Australia microbialite and water samples based on SSU rRNA signatures (cDNA template). Y-axis corresponds to fraction

of OTUs affiliating with each grouping out of 100%. S=smooth mat, C=colloform, P=Pustular, SS=smooth Scoured, SB Water=Shark Bay (Hamelin Pool) waters at microbialite sampling site, and BH Water=coastal enclosed sulfidic water body behind beach on Hamelin Pool, ~20km from microbialite sampling site.

Figure 7. Biplot generated from Cannonical Correspondence Analysis (CCA) of our 18S rRNA data set from Hamelin Pool, Australia for all eukaryotes clustered at the 97% sequence identity level. Sampled microbialite types are circled. Depths of each sample are noted. Filled circles represent 0-1cm fractions, and hollow circles represent 1-2 cm fractions. S=smooth mat, C=colloform mat, P=pustular mat, and SS=smooth Scoured mat.

Figure 8. Unifrac analysis of Hamelin Pool and Highborne Cay samples. Hamelin Pool mat identifiers: 1 and 2=S=smooth mat, 0-1 and 1-2cm depths, 3 and 4=C=colloform mat, 0-1 and 1-2cm depths, 5=pustular mat, 0-1 cm depth, and 6=Shark Bay (Hamelin Pool) water, 7=Blue Hole water, 8=smooth Scoured mat 0-1cm depth. Highborne mat identifiers: 1 and 2=Type 2 mat, 0-1 and 1-2cm depths, 3 and 4=Incipient Type 2 mat 0-1cm and 1-2cm depths, 5=thrombolite 0-1cm depth, 6=Incipient Type 2 mat 0-1cm depth, 7=Type 1 mat 0-1cm depth, 8=thrombolite 1-2cm depth, 9=Type 1 mat 1-2cm depth.

Supplementary Figure 1. Stacked histogram of ciliate OTU composition of (97% sequence similarity, weighted data presentation) in Highborne Cay, Bahamas microbialite samples based ciliate on SSU rRNA signatures (cDNA template). Y-axis corresponds to fraction of OTUs affiliating with each taxonomic grouping out of 100%.

Supplementary Figure 2. Stacked histogram of alveolate taxonomic composition (OTUs at 97% sequence similarity, unweighted data presentation) in Hamelin Pool microbialite and water samples based on SSU rRNA signatures (cDNA template). Y-axis corresponds to fraction of OTUs affiliating with each taxonomic grouping out of 100%. S=Smooth mat, C=colloform, P=pustular, SS=smooth scoured, SB Water=Shark Bay (Hamelin

Pool) waters at microbialite sampling site, and BH Water=coastal enclosed sulfidic water body behind beach on Shark Bay, ~20km from microbialite sampling site.

Supplementary Figure 3. Stacked histogram of stramenopile taxonomic composition (OTUs at 97% sequence similarity, unweighted data presentation) in Hamelin Pool microbialite and water samples based on SSU rRNA signatures (cDNA template). Y-axis corresponds to fraction of OTUs affiliating with each grouping out of 100%. S=smooth mat, C=colloform, P=pustular, SS=smooth scoured, SB Water=Shark Bay (Hamelin Pool) waters at microbialite sampling site, and BH Water=coastal enclosed sulfidic water body behind beach on Shark Bay, ~20km from microbialite sampling site.

Supplementary Figure 4. Stacked histogram of foraminiferal OTU composition of (97% sequence similarity, unweighted data presentation) in Hamelin Pool, Australia, microbialite and water samples based on SSU rRNA signatures (cDNA template). Y-axis corresponds to fraction of OTUs affiliating with each taxonomic grouping out of 100%. S=smooth mat, C=colloform, P=pustular, SS=smooth Scoured, SB Water=Shark Bay (Hamelin Pool) waters at microbialite sampling site, and BH Water=coastal enclosed sulfidic water body behind beach on Shark Bay, ~20km from microbialite sampling site.

Supplementary Figure 5. Heatmap of foraminiferal OTUs (97% sequence similarity) from Hamelin Pool, Australia. Y axis represents log transformed abundance. P=pustular mat, C=colloform mat, SB water=Shark Bay (Hamelin Pool) water above microbialite sampling site, BH water=coastal enclosed sulfidic water body behind beach on Shark Bay, ~20km from microbialite sampling site, S=smooth mat, SS=smooth scoured mat.

Supplementary Figure 6. Biplot generated from Cannonical Correspondence Analysis (CCA) of our combined 18S rRNA data sets from Hamelin Pool, Australia and Highborne Cay, Bahamas, for all eukaryotes clustered at the 97% sequence identity level. Depths of each sample are noted. Hollow circles represent Hamelin Pool samples: S=smooth mat, C=colloform mat, P=pustular mat, and SS=smooth Scoured mat. Filled

617 circles represent Highborne Cay sample types noted for each (note: Type 1-2=Incipient
618 Type 2 mat, Throm=Thrombolite).
619
620

REFERENCES

Admiraal W, Pelletier H. (1979). Sulphide tolerance of benthic ditoms in relation to their distribution in an estuary. *Brit Phycol J* **14**:185-196.

Al-Qassab S, Lee WJ, Murray S, Simpson AGB, Patterson DJ (2002). Flagellates from stromatolites and surrounding sediments in Shark Bay, Western Australia. *Acta Protozoologica* **41:** 91-144.

Allwood AC, Walter MR, Kamber BS, Marshall CP, Burch IW (2006). Stromatolite reef from the Early Archaean era of Australia. *Nature* **441:** 714-718.

Baumgartner LK. 2007. *Diversity and lithification in microbial mats and stromatolites*. PhD dissertation, University of Connecticut, 55-74.

Baumgartner LK, Spear JR, Buckley, DH, Pace, NR, Reid RP, Visscher, PT. (2009). Microbial diversity in modern marine stromatolites, Highborne Cay, Bahamas. *Environmental Microbiology*, **11**:2710–2719.

Baumgartner LK., Reid RP., Dupraz C, Decho AW, Buckley DH, Spear JR, *et al.* (2006). Sulfate reducing bacteria in microbial mats: changing paradigms, new discoveries. *Sediment. Geol*. **185**:131-145.

Bernhard JM. (2003). Potential symbionts in bathyal foraminifera. *Science* **299:** 861-861.

Bernhard JM, Edgcomb VP, Visscher PT, McIntyre-Wressnig A, Summons RE, Bouxsein M, *et al*. (2013). Insights into foraminiferal influences on microfabrics of microbialites at Highborne Cay, Bahamas. *PNAS* doi:10.1073/pnas.1221721110.

Bernhard JM, Habura A, Bowser SS. (2006). An endobiont-bearing allogromiid from the Santa Barbara Basin: Implications for the early diversification of foraminifera. *Journal of Geophysical Research-Biogeosciences* **111**.

Bernhard JM, and Bowser SS. (1992). Bacterial biofilms as a trophic resource for certain benthic foraminifera. *Marine Ecology Progress Series*, **83**: 263-272.

Brehm U, Palinska KA, Krumbein WE. (2004). Laboratory cultures of calcifying biomicrospheres generate ooids – A contribution to the origin of oolites. *Carnets de Geologie/Notebooks on Geology, Maintenon, Letter* 2004/03:1-6.

Burki F, Inagaki Y, Brate J, Archibald JM, Keeling PJ, Cavalier-Smith T, *et al*. (2009). Large-scale phylogenomic analyses reveal that two enigmatic protist lineages, Telonemia and Centroheliozoa, are related to photosynthetic chromalveolates. *Genome Biol and Evol* doi: 10.1093/gbe/evp022.

Burns BP, Goh F, Allen M, Neilan, BA. (2004). Microbial diversity of extant stromatolites in the hypersaline marine environment of Shark Bay, Australia. *Env Microbiol* **6**:1096-1101.

Caporaso JG, Kuczynski J, Strombaugh J, Bittinger K, Bushman FD, Costello EK, *et al.* (2010). QIIME allows analysis of high-throughput community sequencing data. *Nat Meth* **7**:335-336.

Cole JR, Chai B, Marsh TL, Farris RJ, Wang Q, Kulam SA *et al*. (2003). The Ribosomal Database Project (RDP-II): previewing a new autoaligner that allows regular updates and the new prokaryotic taxonomy. *Nucleic Acids Res* **31**: 442–443.

Couradeau E, Benzerara K, Moreira D, Gerard E, Kazmierczak J, Tavara R, *et al*. (2011). Prokaryotic and eukaryotic community structure in field and cultured microbialites from the alkaline lake Alchichica (Mexico). *PLoS One* **6**(12): e28767, doi: 10.1371/journal.pone.0028767.

Davaud E, Girardclos S. (2001). Recent freshwater ooids and oncoids from western Lake Geneva (Switzerland): Indications of a common organically mediated origin. *J. Sedimentary Res*. **71**:423-429.

Davies, PJ, Bubela B, Ferguson J. (1978). The formation of ooids. *Sedimentology* **25**(5):703-729.

Donohue J. (1969). Genesis of oolite and posolite grains: an energy index. *J. Sedimentary Petrology* **39**(4):1399-1411.

Duguid SMA, Kyser K, James NP, Rankey EC. (2010). Microbes and ooids. *J. Sedimentary Res*. **80**:236-251.

Dupraz C, Visscher PT. (2005). Microbial lithification in marine stromatolites and hypersaline mats. *Trends in Microbiology* **13**(9):429-438.

Farmer JD. (1992). Grazing and bioturbation in modern microbial mats. In: J.W. Schopf & C. Klein, *The Proterozoic Biosphere – A multidisciplinary Study*. Cambridge University Press, pp. 295-297.

Feazel LM, Spear JM, Berger AB, Harris JK, Frank DN, Ley RE, Pace NR. (2008). Eucaryotic diversity in a hypersaline microbial mat. *Appl. Environ. Microbiol.* **74(1)**:329-332.

Feldmann M, McKenzie JA (1998). Stromatolite-thrombolite associations in a modern environment, Lee Stocking Island, Bahamas. *Palaios* **13**, 201–212.

Fenchel T, Finlay B. (1995). *Ecology and Evolution in Anoxic Worlds*. Oxford.

712
713 Folk RL, Lynch FL. (2001). Organic matter, putative nannobacteria and the formation of
714 ooids and hardgrounds. *Sedimentology* **8**:215-229.
715
716 Foster JS, Green SJ. (2011). Microbial diversity in modern stromatolites. In V.C. Tewari
717 and J. Seckbach (eds.) Stromatolites: Interaction of Microbes with Sediments,
718 *Cellular Origin, Life in Extreme Habitats and Astrobiology* **18**:383-405.
719
720 Foster JS, Green SJ, Ahrendt SR, Golubic S, Reid RP, Hetherington KL, *et al*. (2009).
721 Molecular and morphological characterization of cyanobacterial diversity in the
722 stromatolites of Highborne Cay, Bahamas. *The ISME J* **3**:573-587.
723
724 Glud RN, Fenchel T. (1999). The importance of ciliates for interstitial solute transport in
725 marine sediments. *Mar Ecol Prog Ser* **186**:87–93.
726
727 Golubic S, Friedmann I, Schneider J. (1981). The lithobiontic ecological niche, with
728 special reference to microorganisms. *J. Sedimentol. Res*. **52**:475-478.
729
730 Gross O. (2002). Sediment interactions of foraminifera: Implications for food degradation
731 and bioturbation processes. *Journal of Foraminiferal Research* **32:** 414-424.
732
733 Grotzinger JP, Knoll AH. (1999). Stromatolites in Precambrian carbonates: Evolutionary
734 mileposts or environmental dipsticks? *Annual Review of Earth and Planetary*
735 *Sciences* **27:** 313-358.
736
737 Guyoneaud R, Moune S, Eatock C, Bothorel V, Hirschler-Rea A. *et al.* (2002).
738 Characterization of three spiral-shaped purple nonsulfur bacteria isolated from
739 coastal lagoon sediments, saline sulfur springs, and microbial mats: emended
740 description of the genus *Roseospira thiosulfatophila* sp. nov. *Arch Microbiol*
741 **178**:315-324.
742
743 Harris PM, Halley RB, Lukas KJ. (1979). Endolith microborings and their preservation in
744 Holocene-Pleistocene (Bahamas-Florida) ooids. *Geology* **7**:216-220.
745
746 Jahnert RL, Collins LB. (2011). Significance of subtidal microbial deposits in Shark Bay,
747 Australia. *Marine Geology* **286**:106-111.
748
749 Jahnert RJ, Collins LB. (2012). Characteristics, distribution and morphogenesis of
750 subtidal microbial systems in Shark Bay, Australia. *Marine Geology* **303-**
751 **306**:115-136.
752
753 Kennard JM, James NP. (1986). Thrombolites and stromatolites: two distinct types of
754 microbial structures. *Palaios* **1**: 492–503.
755
756 Logan BW. (1961). Cryptozoon and associate stromatolites from the Recent, Shark Bay,
757 Western Australia. *J Geology* **69**(5):517–533.

Mastandrea A, Perri E, Russo F, Spadafora A, Tucker M (2006). Microbial primary dolomite from a Norian carbonate platform: northern Calabria, southern Italy. *Sedimentology* **53:** 465-480.

Mitterer RM. (1972). Biogeochemistry of aragonite mud and oolites. *Geochimica et Cosmochimica Acta* **36**:1407-1422.

Moon-van der Staay SY, De Wachter R, Vaulot D. (2001). Oceanic 18S rDNA sequences from picoplankton reveal unsuspected eukaryotic diversity. *Nature* **409**: 607-610.

Myshrall KL, Mobberley JM, Green SJ, Visscher PT, Havemann SA, Reid RP *et al* (2010). Biogeochemical cycling and microbial diversity in the thrombolitic microbialites of Highborne Cay, Bahamas. *Geobiology* **8:** 337-354.

Nagai S, Imai I. (1999). Factors inducing resting-cell formation of *Coscinodiscus wailesii* Gran (Bacillariophyceae) in culture. *Plankton Biol* **46**:94-103.

Nebel ME, Wild S, Holzhauser M, *et al*. (2011). Jaguc – a software package for environmental diversity analyses. *Journal of Bioinformatics and Computational Biology* **9(6):** 749-73.

Papineau D, Walker JJ, Mojzsis SJ, Pace NR (2005). Composition and structure of microbial communities from stromatolites of Hamelin Pool in Shark Bay, Western Australia. *Applied and Environmental Microbiology* **71:** 4822-4832.

Pawlowski J. (2000). Introduction to the molecular systematics of foraminifera. *Micropaleontology*; **46**, (supplement no1) 1-1.

Pike J, Bernhard JM, Moreton SG, Butler IB. (2001). Microbioirrigation of marine sediments in dysoxic environments: implications for early sediment fabric formation and diagenetic processes. *Geology*, **29**: 923-926.

Planavsky N, Ginsburg RN. (2009). Taphonomy of modern marine Bahamian microbialites, *Palaios*, **24**(1):5-17.

Planavsky N, Reid RP, Lyons TW, Myshrall PT, Visscher PT. (2009). Formation and diagenesis of modern marine calcified cyanobacteria. *Geobiology* **7**(5):566-576.

Plee K, Pacton M, Ariztegui D. (2010). Discriminating the role of photosynthetic and heterotrophic microbes triggering low-Mg calcite precipitation in freshwater biofilms (Lake Geneva, Switzerland). *Geomicrobiology* J. **27**:391-399.

Pusch M, Fiebig D, Brettar I, Eisenmann H, Ellis BK, Kaplan LA, *et al.* (1998). The role of micro-organisms in the ecological connectivity of running waters. *Freshwater Biology* **40**:453-495.

Quince C, Lanzen A, Curtis TP, Davenport RJ, Hall N, Head IM, *et al*. (2009). Accurate determination of microbial diversity from 454 pyrosequencing data. *Nat Methods*.**6**:639–641.

Raghukumar S. (2002). Ecology of the marine protists, the Labyrinthulomycetes (Thraustochytrids and Labyrinthulids). *Eur J Protistol* **38**:127-145.

Reichardt W. (1988). Effect of bioturbation by *Arenicola marina* on microbiological parameters in intertidal sediments. *Mar Ecol – Prog Ser* **44**:149-158.

Reid RP, Visscher PT, Decho AW, Stolz JF, Bebout BM, Dupraz C. *et al.* (2000). The role of microbes in accretion, lamination, and early lithification of modern marine stromatolites. *Nature* **406**:989-992.

Stal LJ (2000). Cyanobacterial mats and stromatolites. In: Whitton BA and Potts M (eds). *The Ecology of Cyanobacteria*. Kluwer Academic. pp 61-120.

Stoeck T, Bass D, Nebel M, Christen R, Jones MD, Breiner HW *et al*. (2010). Multiple marker parallel tag environmental DNA sequencing reveals a highly complex eukaryotic community in marine anoxic water. *Mol Ecol* **19**(Suppl 1): 21–31.

Stolz JF, Feinstein TN, Salsi J, Visscher PT, Reid RP. (2001). TEM analysis of microbial mediated sedimentation and lithification in modern marine stromatolites. *Am. Minerol* **86**:826-833.

Thompson JB, Ferris FG, Smith DA. (1990). Geomicrobiology and sedimentology of the mixolimnion and chemocline in Fayetteville Green Lake, New York. *Palaios* **5**, 52–75.

Tucker ME, Wright VP. (1990). *Carbonate Sedimentology*. Blackwell Science.

Vd'ačny P, Bourland WA, Orsi W, Epstein SS, Foissner W. (2011). Phylogeny and classification of the Litostomatea (Protista, Ciliophora), with emphasis on free-living taxa and the 18S rRNA gene. Mol Phylogen Evol **59**:510-522.

Visscher PT, Stolz, JF. (2005). Microbial mats as bioreactors: populations, processes and products. *Palaeogeogr. Palaeoclimatol. Palaeoecol*. 219:87-100.

Visscher PT, Reid RP, Bebout BM, Hoeft SE, Macintyre IG, Thompson JA. (1998) Formation of lithified micritic laminae in modern marine stromatolites (Bahamas): the role of sulfur cycling. *American Mineralogist* **83**:1482–1493.

Walter MR, Heys GR. (1985). Links between the rise of the metazoa and the decline of stromatolites. *Precambrian Research* **29:** 149-174.

Westphalen D. (1993). Stromatolitoid microbial nodules from Bermuda – A microhabitat for meiofauna. *Marine Biology* **117:** 145-157.

Table 1. Temperature, Salinity, Oxygen, Sulfide, Temperature and Salinity data for Hamelin Pool, Australia and Highborne Cay, Bahamas microbialite samples. n/a = not observed. For sulfide data, depth noted is where free sulfide ($H_2S/HS^-/S^{2-}$) is first observed, and the maximum concentration during the day during sampling is based on single profiles (note: replicate profiles are very similar). Oxygen data are presented as the ranges of maximum depth and maximum % oxygen saturation in each sample.

Highborne Cay	**Temperature**	**Salinity (PSU)**	**Max. % O_2 Saturation (depth in mm)**	**Sulfide(µM) (depth first observed in mm)**
Type 1 mat 0-1cm	25.4-25.9°C	33-35.5	225-264 (2.2-2.4mm)	n/a
Type 1 mat 1-2cm	25.4-25.9°C	33-35.5	0 (0mm)	24 (12.25)
Type 2 mat 0-1cm	25.4-25.9°C	33-35.5	394-456 (5.8-6.4)	76 (7.25)
Type 2 mat 1-2cm	25.4-25.9°C	33-35.5	0 (0)	282 (throughout)
Incipient Type II mat 0-1cm	25.4-25.9°C	33-35.5	285-346 (7.4-8.2)	17 (9.25mm)
Incipient Type II mat 1-2cm	25.4-25.9°C	33-35.5	0 (0)	192 (throughout)
Thrombolite 0-1cm	25.4-25.9°C	33-35.5	536-622 (8.2-9.6)	10 (9.75)
Thrombolite 1-2cm	25.4-25.9°C	33-35.5	0 (0)	168 (throughout)
Highborne water	25.4-25.9°C	33-35.5	100	n/a
Hamelin Pool				
Pustular mat 0-1cm	14-15°C	66-72	174-218 (5.8-6.4)	38 (6.25)
Pustular mat 1-2cm	14-15°C	66-72	0 (0)	81 (throughout)
Colloform mat 0-1cm	14-15°C	66-72	188-230 (5.8-6.2)	19 (7.75)
Colloform mat 1-2cm	14-15°C	66-72	0 (0)	189 (throughout)
Smooth mat 0-1 cm	14-15°C	66-72	229-312 (7.4-8.2)	26 (7.5)

Smooth mat 1-2cm	14-15°C	66-72	0 (0)	170 (throughout)
Smooth Scoured mat 0-1cm	14-15°C	66-72	100-108 (2.6-3.4)	32 (4.0mm)
Smooth Scoured mat 1-2cm	14-15°C	66-72	0 (0)	76 (throughout)
Hamelin Pool water	14-15°C	66-72	100	n/a
Blue Hole sulfidic water	18°C	78	0	n/a

Table 2. Multi Response Permutation Procedure (MRPP) P values for sample parameters for Highborne Cay (HC), Hamelin Pool (HP) and combined data sets. MRPP values are combined for depth and oxygen for all data sets because all 0-1cm samples were oxic and all 1-2cm samples were anoxic. na=not applicable.

	Depth/Oxygen	**Site**	**Mat Type**	**Salinity**
HC-all eukaryotes	0.455	na	0.028	na
HC-foraminfera	0.027	na	0.776	na
HP-all eukaryotes	0.817	na	0.000	na
HP-foraminifera	0.001	na	0.000	na
Combined-all eukaryotes	0.061	0.001	0.001	<0.001
Combined-foraminfera	0.051	0.007	0.055	na

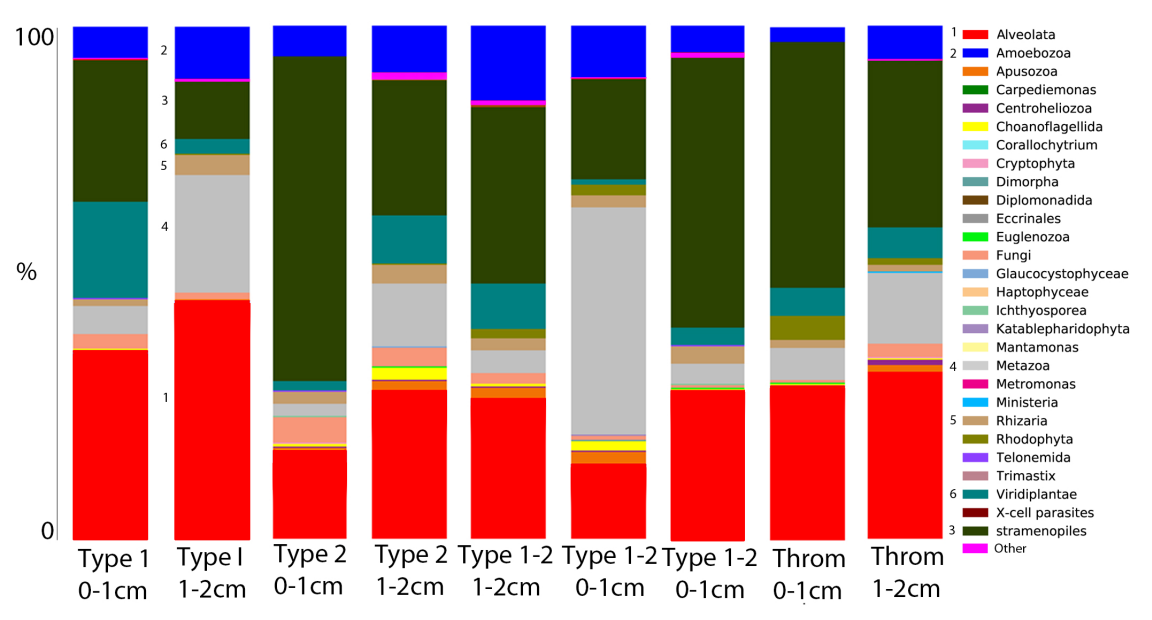
100
%
0
Type 1 0-1cm
Type I 1-2cm
Type 2 0-1cm
Type 2 1-2cm
Type 1-2 1-2cm
Type 1-2 0-1cm
Type 1-2 0-1cm
Throm 0-1cm
Throm 1-2cm
1 Alveolata
2 Amoebozoa
Apusozoa
Carpediemonas
Centroheliozoa
Choanoflagellida
Corallochytrium
Cryptophyta
Dimorpha
Diplomonadida
Eccrinales
Euglenozoa
Fungi
Glaucocystophyceae
Haptophyceae
Ichthyosporea
Katablepharidophyta
Mantamonas
4 Metazoa
Metromonas
Ministeria
5 Rhizaria
Rhodophyta
Telonemida
Trimastix
6 Viridiplantae
X-cell parasites
3 stramenopiles
Other

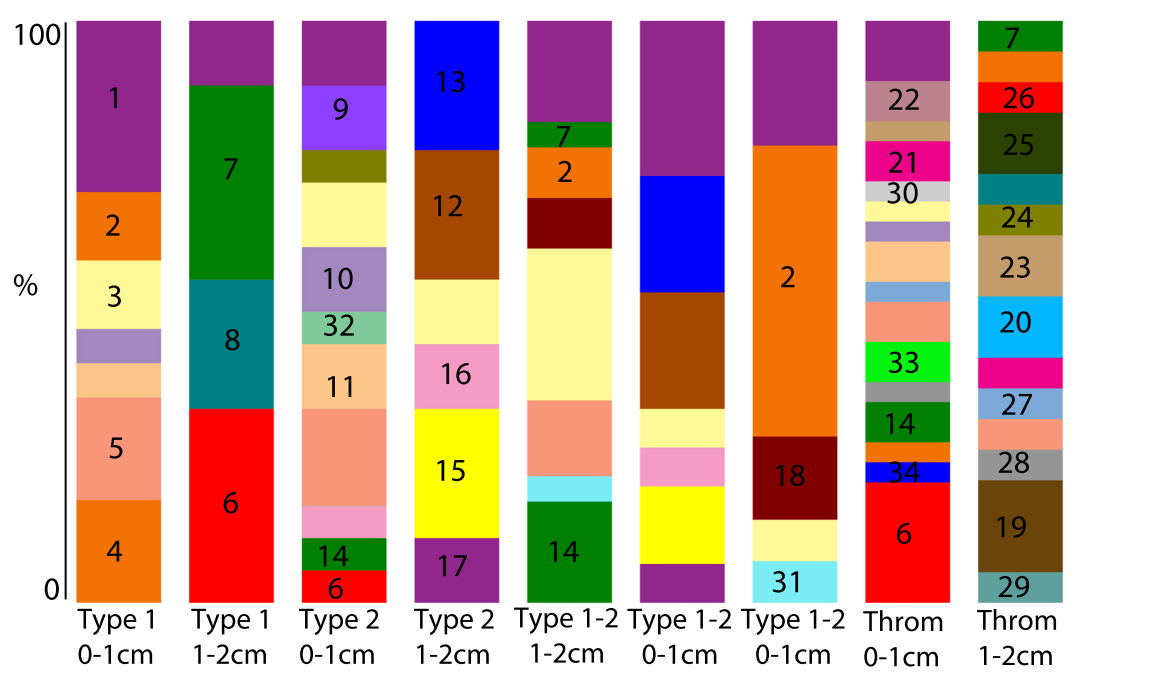
100
%
0
Type 1 0-1cm
Type 1 1-2cm
Type 2 0-1cm
Type 2 1-2cm
Type 1-2 1-2cm
Type 1-2 0-1cm
Type 1-2 0-1cm
Throm 0-1cm
Throm 1-2cm
6 Allogromida;unclassified Allogromida
34 Miliolina;Alveolinidae;Borelis
4 Miliolina;Hauerinidae;Pyrgo
14 Miliolina;Miliolidae;Quinqueloculininae;Quinqueloculina
17 Miliolina;Peneroplidae;Spirolina
15 Miliolina;Soritidae;Archaiasinae;Androsina
31 Miliolina;Soritidae;Laevipeneroplis
16 Rotaliida;Bolivinacea;Bolivinidae;Bolivina
29 Rotaliida;Buliminacea;Uvigerinidae;Uvigerina
19 Rotaliida;Cassidulinacea;Cassidulinidae;Cassidulinoides
28 Rotaliida;Cibicididae;Cibicides
33 Rotaliida;Discorbacea;Discorbidae;Cancris
5 Rotaliida;Discorbacea;Discorbidae;Discorbis
27 Rotaliida;Discorbacea;Glabratellidae;Angulodiscrobis
11 Rotaliida;Discorbacea;Glabratellidae;Glabratella
32 Rotaliida;Discorbacea;Rosalinidae;Rosalina
10 Rotaliida;Discorbinellacea;Pseudoparrellidae;Epistominella
3 Rotaliida;Elphidiidae;Elphidium
30 Rotaliida;Globigerinacea;Globigerinidae;Globigerinita
21 Rotaliida;Nonionacea;Anomalinidae;Cibicidoides
20 Rotaliida;Nonionacea;Nonionidae;Haynesina
23 Rotaliida;Nonionacea;Nonionidae;Nonionella
24 Rotaliida;Nummulitidae;Nummulites
9 Rotaliida;Nummulitidae;Planostegina
22 Rotaliida;Planorbulinacea;Planorbulinidae;Planorbulina
8 Rotaliida;Planorbulinacea;Planorbulinidae;Planorbulinella
18 Rotaliida;Rotaliacea;Rotaliidae;Ammonia
25 Rzehakinidae;Miliammina
12 Spirillinida;Patellinidae;Patellina
26 Textulariida;Astrorhizida;Bathysiphonidae;Bathysiphon
13 Textulariida;Astrorhizida;Saccamminidae;Hippocrepinella
2 Textulariida;Textulariacea;Eggerellidae;Eggerelloides
7 Textulariida;Trochamminacea;Trochamminidae;Trochammina
1 Other

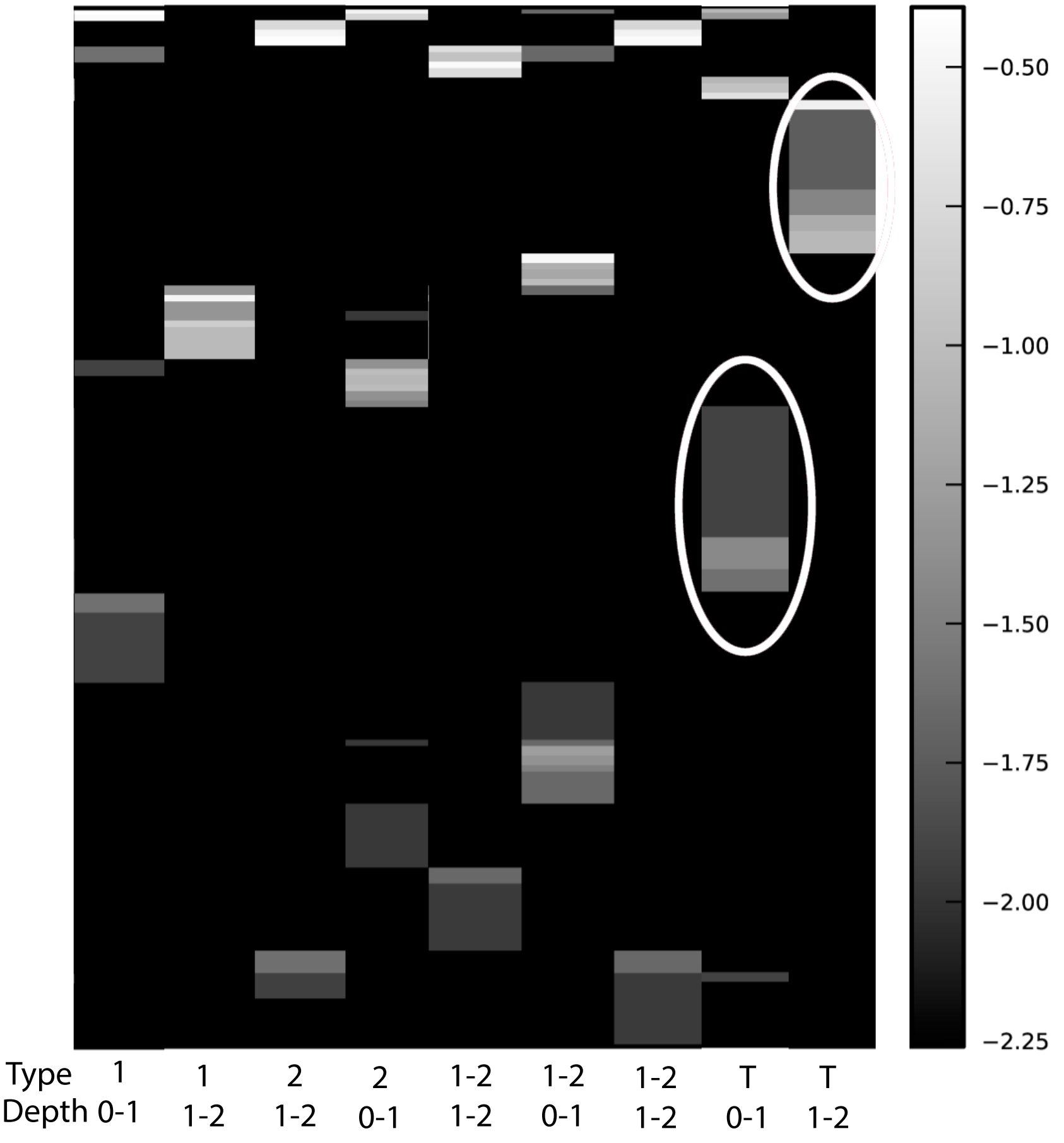
−0.50
−0.75
−1.00
−1.25
−1.50
−1.75
−2.00
−2.25
Type 1 1 2 2 1-2 1-2 1-2 T T
Depth 0-1 1-2 1-2 0-1 1-2 0-1 1-2 0-1 1-2

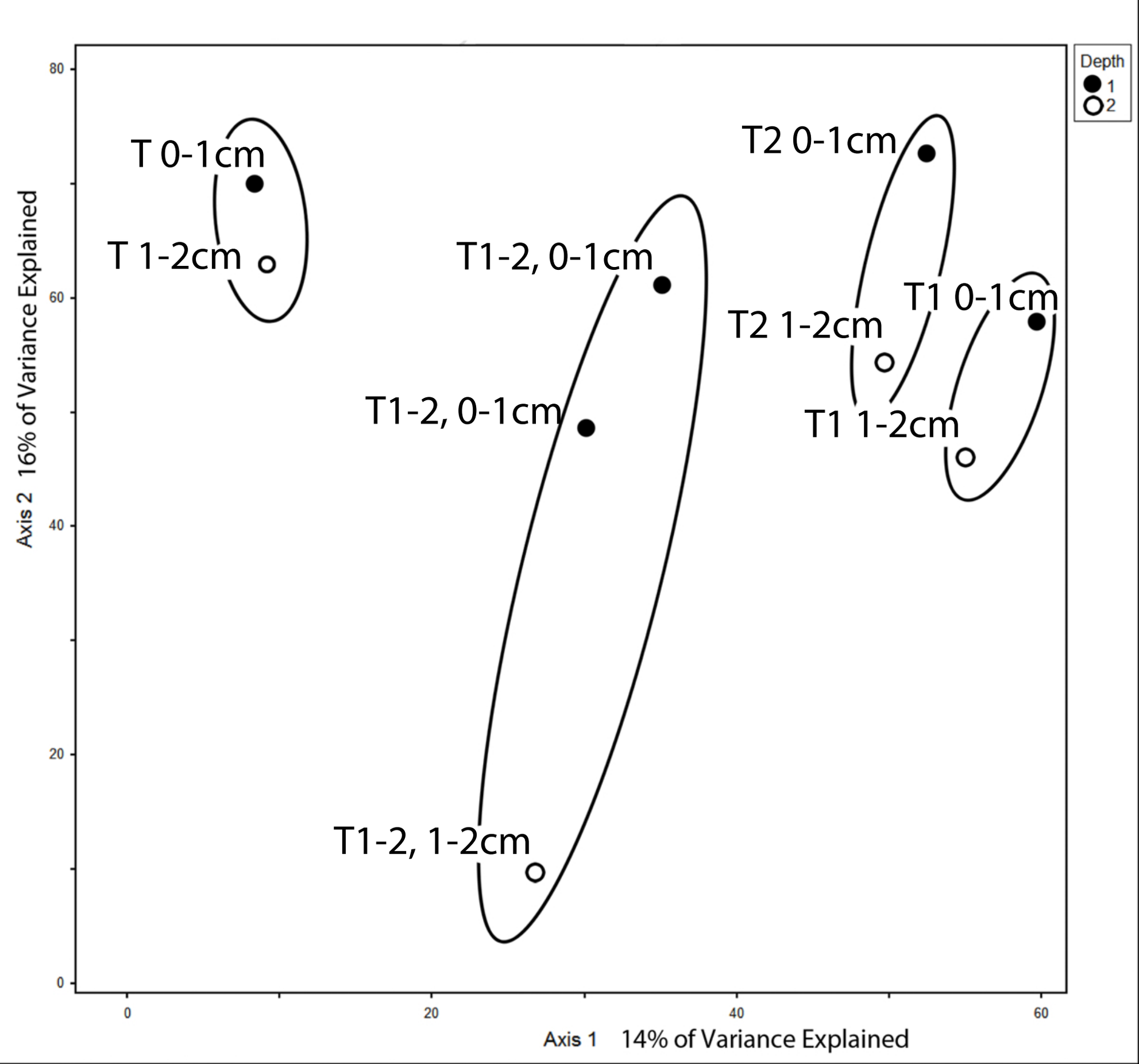
Depth
1
2
T 0-1cm
T 1-2cm
T1-2, 0-1cm
T1-2, 0-1cm
T1-2, 1-2cm
T2 0-1cm
T2 1-2cm
T1 0-1cm
T1 1-2cm
Axis 2 16% of Variance Explained
Axis 1 14% of Variance Explained
0
20
40
60
80
0
20
40
60

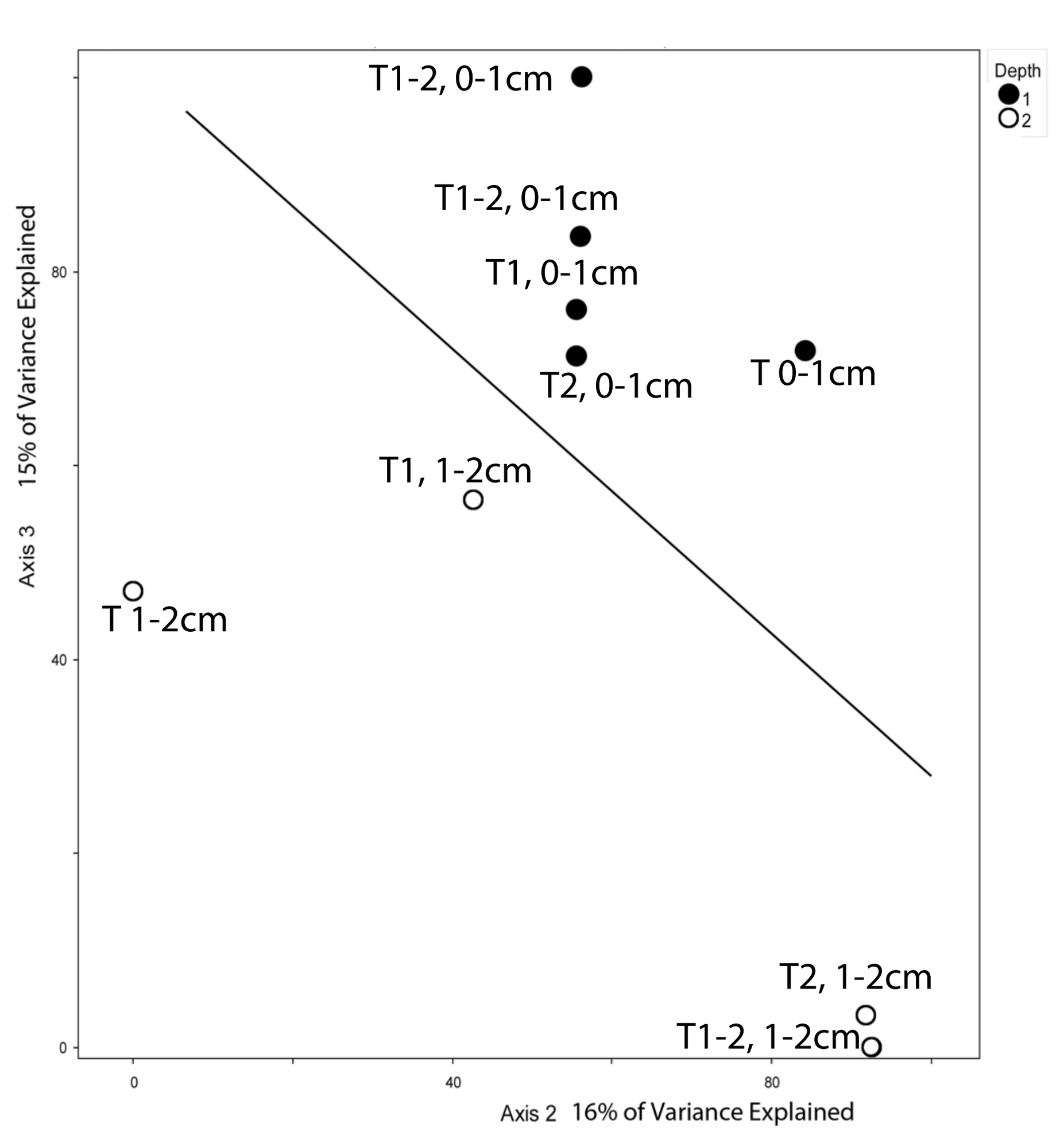
Depth
1
2
T1-2, 0-1cm
T1-2, 0-1cm
T1, 0-1cm
T2, 0-1cm
T 0-1cm
T1, 1-2cm
T 1-2cm
T2, 1-2cm
T1-2, 1-2cm
Axis 3 15% of Variance Explained
0
40
80
0
40
80
Axis 2 16% of Variance Explained

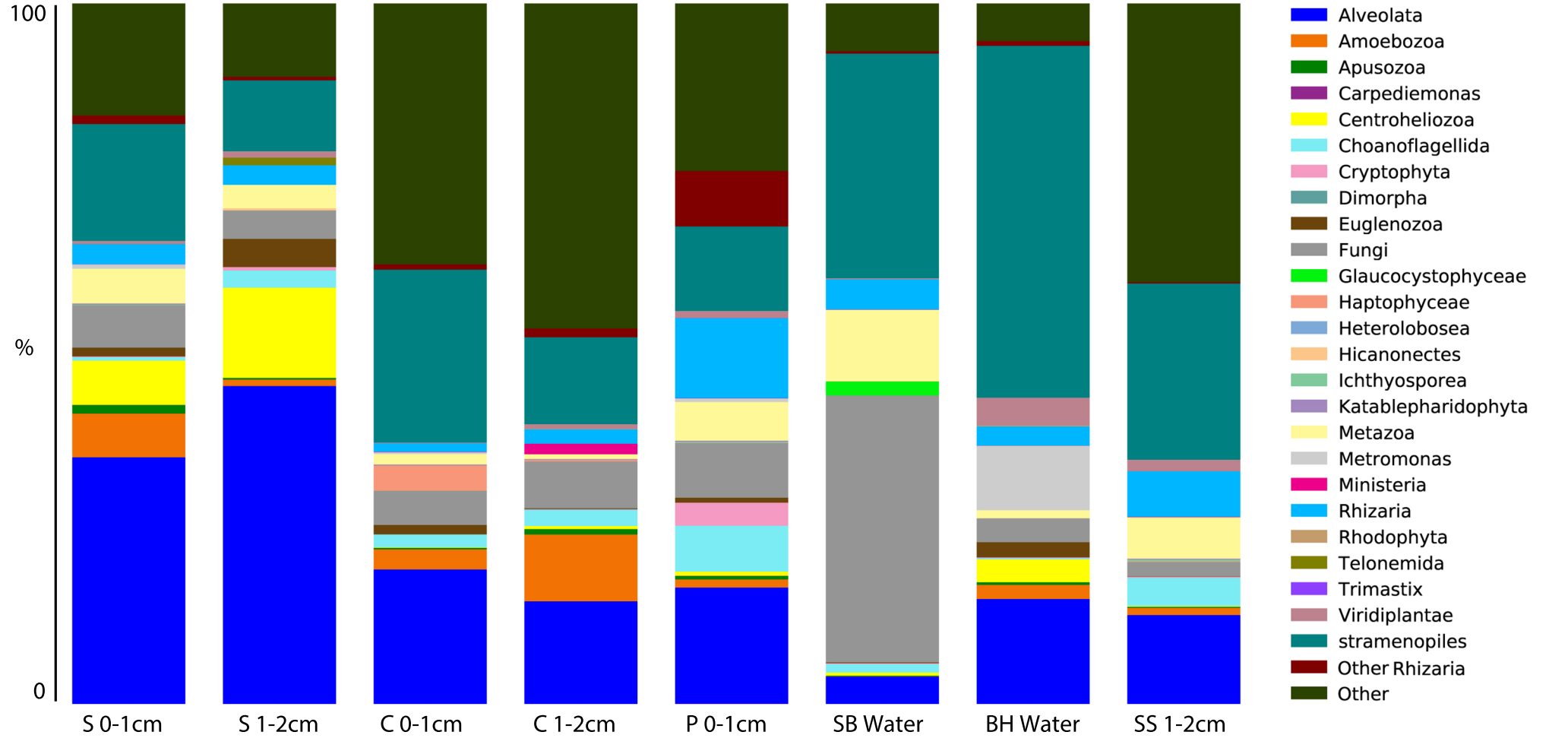
100
%
0
S 0-1cm
S 1-2cm
C 0-1cm
C 1-2cm
P 0-1cm
SB Water
BH Water
SS 1-2cm
Alveolata
Amoebozoa
Apusozoa
Carpediemonas
Centroheliozoa
Choanoflagellida
Cryptophyta
Dimorpha
Euglenozoa
Fungi
Glaucocystophyceae
Haptophyceae
Heterolobosea
Hicanonectes
Ichthyosporea
Katablepharidophyta
Metazoa
Metromonas
Ministeria
Rhizaria
Rhodophyta
Telonemida
Trimastix
Viridiplantae
stramenopiles
Other Rhizaria
Other

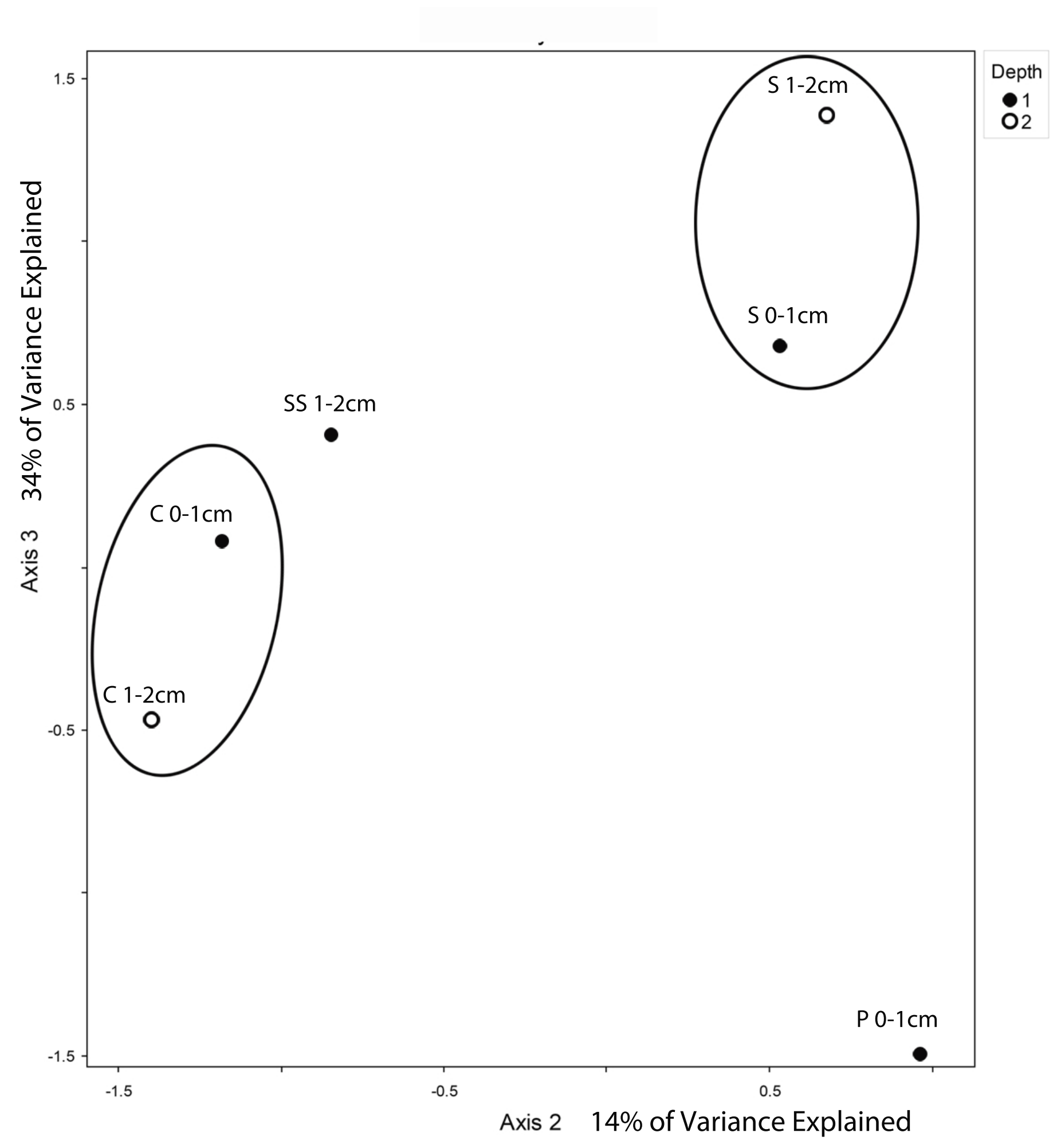
Depth
1
2
S 1-2cm
S 0-1cm
SS 1-2cm
C 0-1cm
C 1-2cm
P 0-1cm
1.5
0.5
-0.5
-1.5
-1.5
-0.5
0.5
Axis 3 34% of Variance Explained
Axis 2 14% of Variance Explained

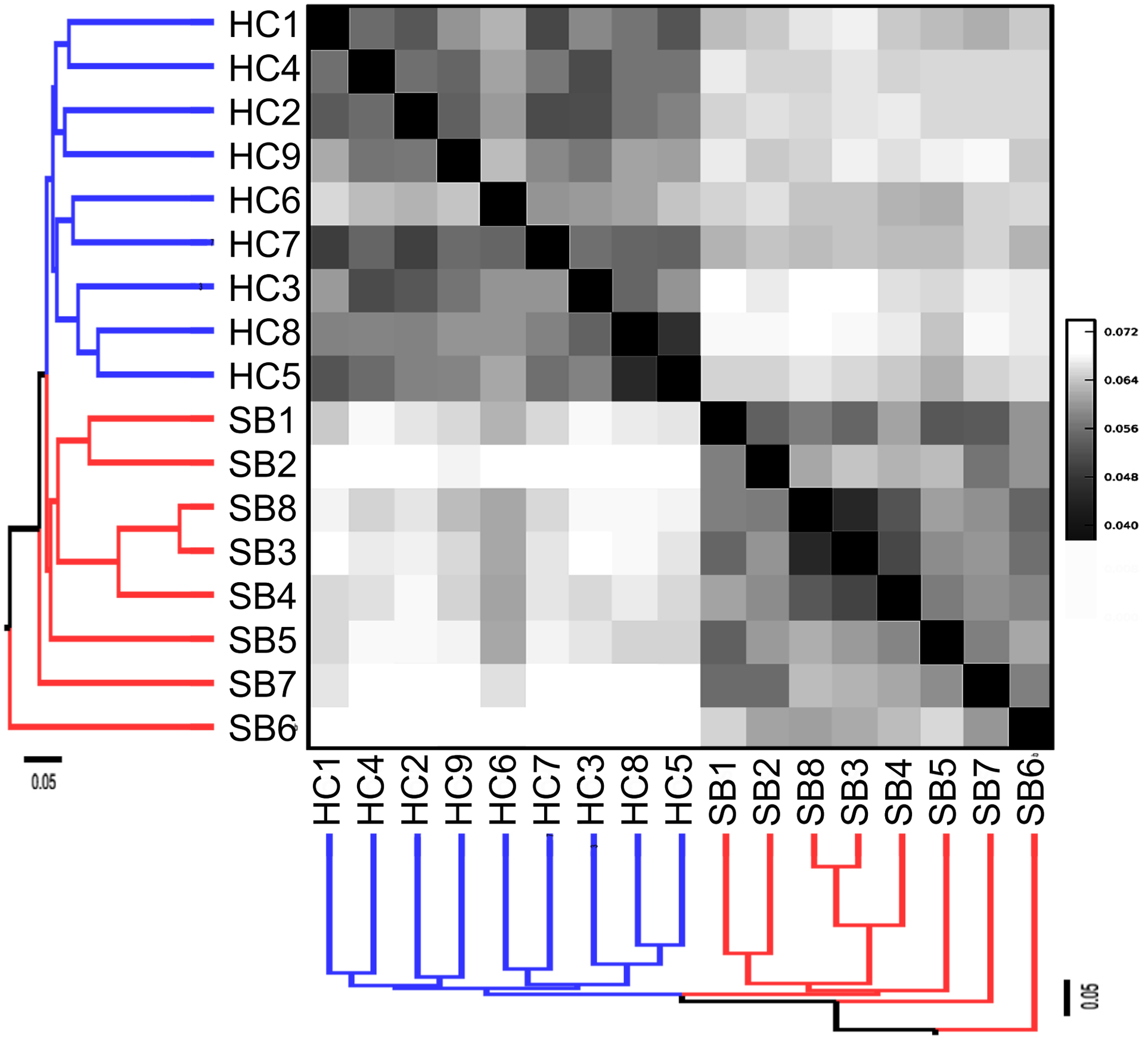
HC1
HC4
HC2
HC9
HC6
HC7
HC3
HC8
HC5
SB1
SB2
SB8
SB3
SB4
SB5
SB7
SB6
0.05
0.072
0.064
0.056
0.048
0.040
HC1
HC4
HC2
HC9
HC6
HC7
HC3
HC8
HC5
SB1
SB2
SB8
SB3
SB4
SB5
SB7
SB6
0.05

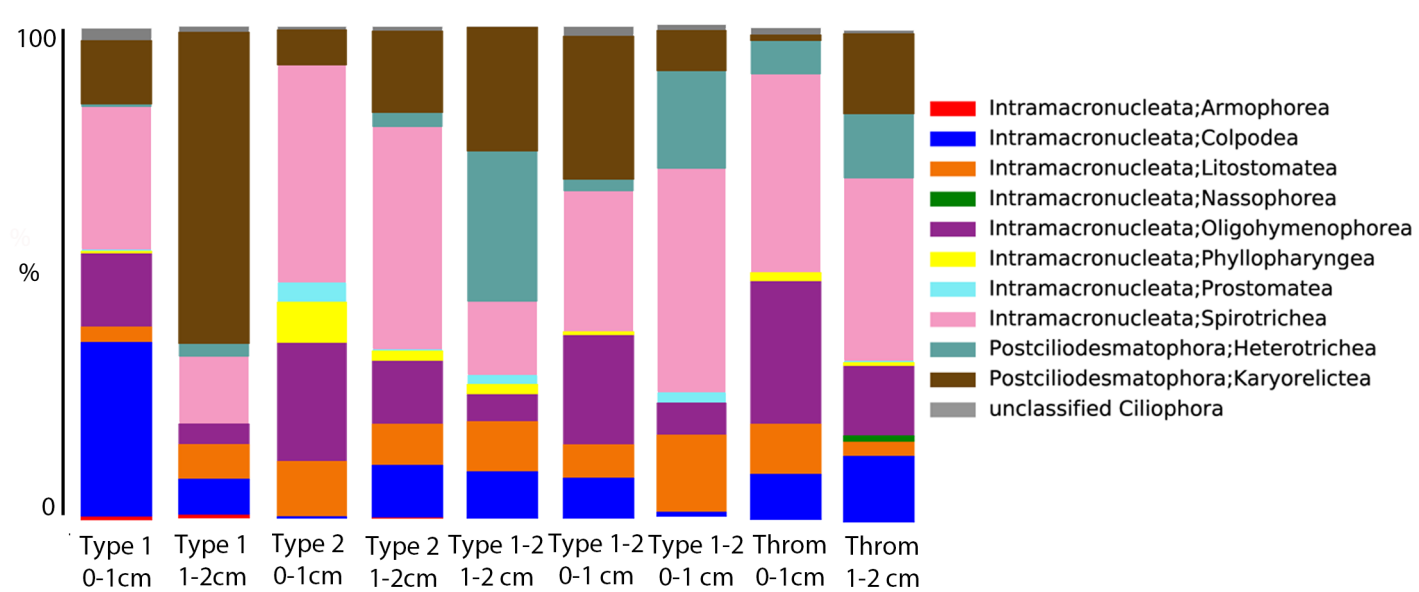
100
%
0
Type 1 0-1cm
Type 1 1-2cm
Type 2 0-1cm
Type 2 1-2cm
Type 1-2 1-2 cm
Type 1-2 0-1 cm
Type 1-2 0-1 cm
Throm 0-1cm
Throm 1-2 cm
Intramacronucleata;Armophorea
Intramacronucleata;Colpodea
Intramacronucleata;Litostomatea
Intramacronucleata;Nassophorea
Intramacronucleata;Oligohymenophorea
Intramacronucleata;Phyllopharyngea
Intramacronucleata;Prostomatea
Intramacronucleata;Spirotrichea
Postciliodesmatophora;Heterotrichea
Postciliodesmatophora;Karyorelictea
unclassified Ciliophora

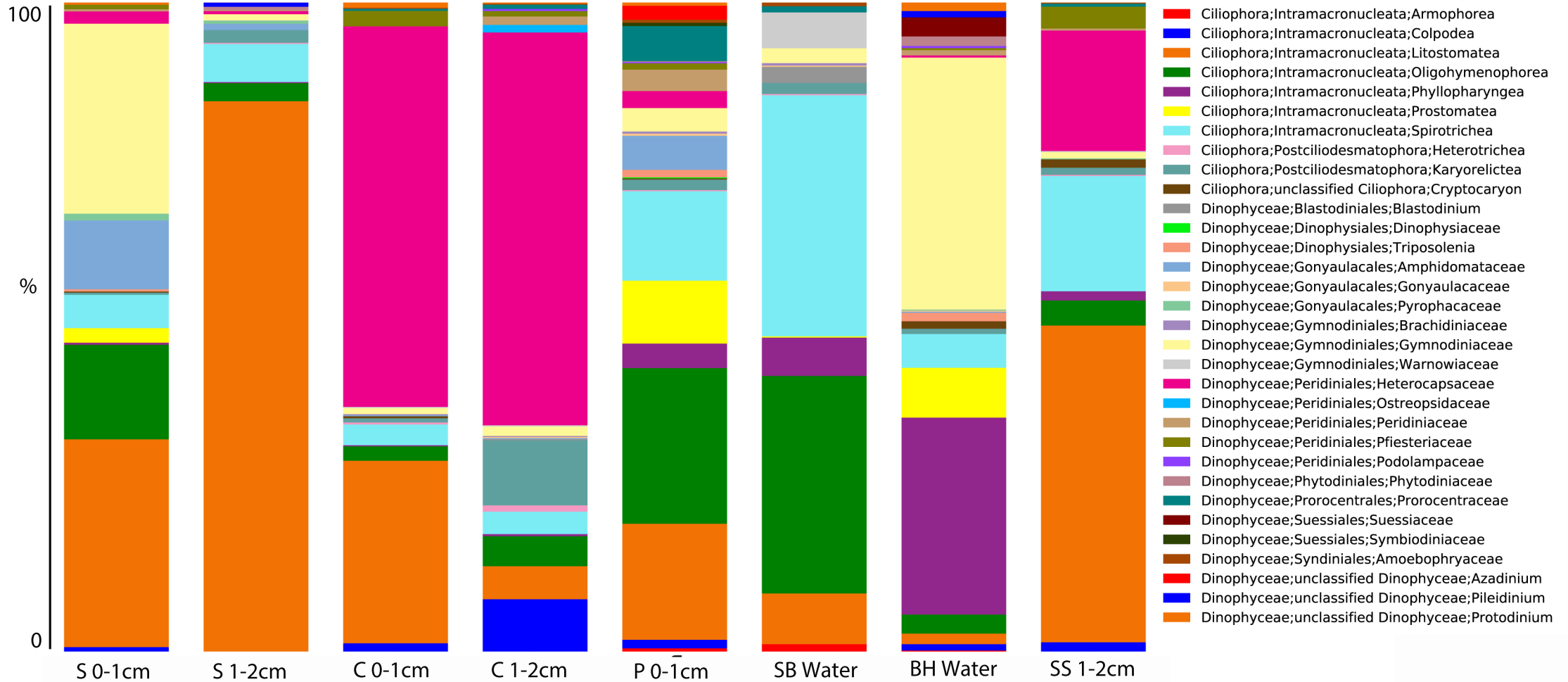
100
%
0
S 0-1cm
S 1-2cm
C 0-1cm
C 1-2cm
P 0-1cm
SB Water
BH Water
SS 1-2cm
Ciliophora;Intramacronucleata;Armophorea
Ciliophora;Intramacronucleata;Colpodea
Ciliophora;Intramacronucleata;Litostomatea
Ciliophora;Intramacronucleata;Oligohymenophorea
Ciliophora;Intramacronucleata;Phyllopharyngea
Ciliophora;Intramacronucleata;Prostomatea
Ciliophora;Intramacronucleata;Spirotrichea
Ciliophora;Postciliodesmatophora;Heterotrichea
Ciliophora;Postciliodesmatophora;Karyorelictea
Ciliophora;unclassified Ciliophora;Cryptocaryon
Dinophyceae;Blastodiniales;Blastodinium
Dinophyceae;Dinophysiales;Dinophysiaceae
Dinophyceae;Dinophysiales;Triposolenia
Dinophyceae;Gonyaulacales;Amphidomataceae
Dinophyceae;Gonyaulacales;Gonyaulacaceae
Dinophyceae;Gonyaulacales;Pyrophacaceae
Dinophyceae;Gymnodiniales;Brachidiniaceae
Dinophyceae;Gymnodiniales;Gymnodiniaceae
Dinophyceae;Gymnodiniales;Warnowiaceae
Dinophyceae;Peridiniales;Heterocapsaceae
Dinophyceae;Peridiniales;Ostreopsidaceae
Dinophyceae;Peridiniales;Peridiniaceae
Dinophyceae;Peridiniales;Pfiesteriaceae
Dinophyceae;Peridiniales;Podolampaceae
Dinophyceae;Phytodiniales;Phytodiniaceae
Dinophyceae;Prorocentrales;Prorocentraceae
Dinophyceae;Suessiales;Suessiaceae
Dinophyceae;Suessiales;Symbiodiniaceae
Dinophyceae;Syndiniales;Amoebophryaceae
Dinophyceae;unclassified Dinophyceae;Azadinium
Dinophyceae;unclassified Dinophyceae;Pileidinium
Dinophyceae;unclassified Dinophyceae;Protodinium

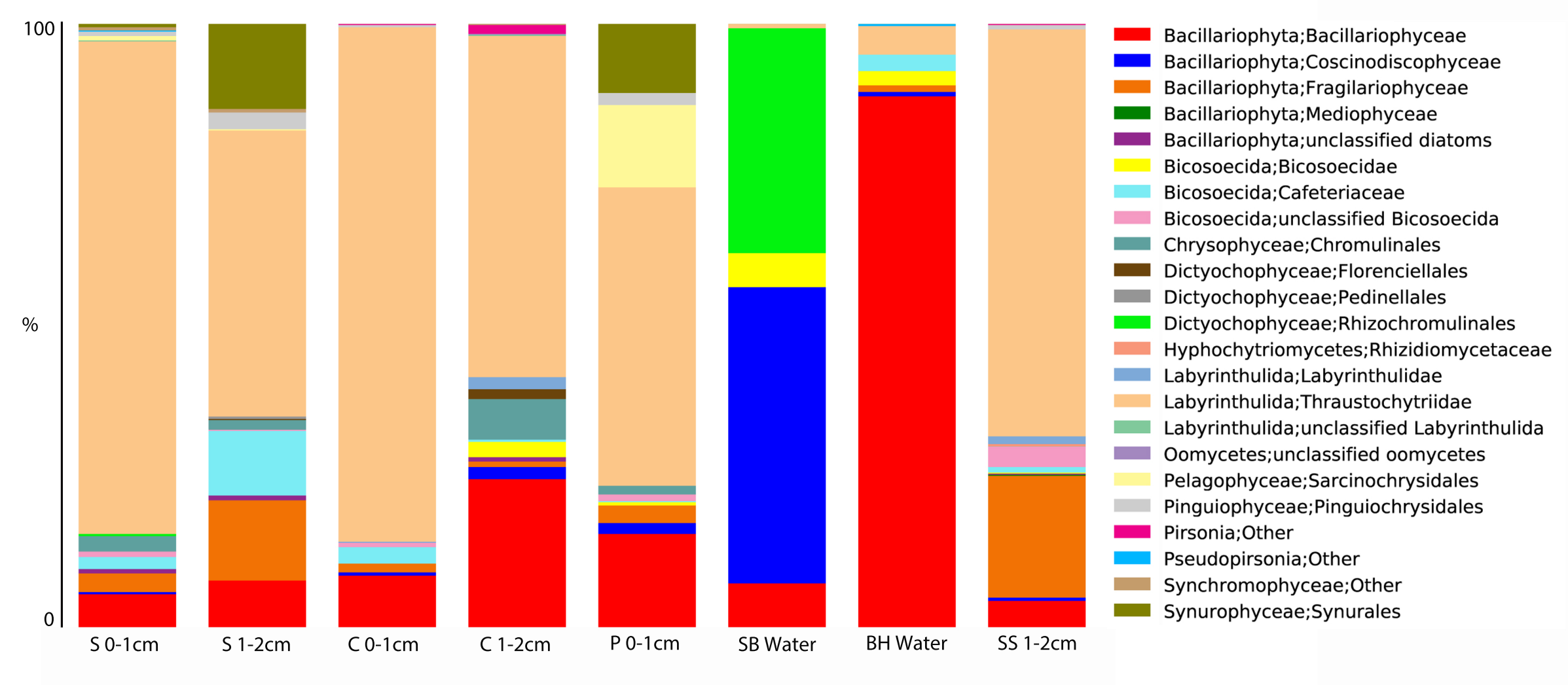
100
%
0
S 0-1cm
S 1-2cm
C 0-1cm
C 1-2cm
P 0-1cm
SB Water
BH Water
SS 1-2cm
Bacillariophyta;Bacillariophyceae
Bacillariophyta;Coscinodiscophyceae
Bacillariophyta;Fragilariophyceae
Bacillariophyta;Mediophyceae
Bacillariophyta;unclassified diatoms
Bicosoecida;Bicosoecidae
Bicosoecida;Cafeteriaceae
Bicosoecida;unclassified Bicosoecida
Chrysophyceae;Chromulinales
Dictyochophyceae;Florenciellales
Dictyochophyceae;Pedinellales
Dictyochophyceae;Rhizochromulinales
Hyphochytriomycetes;Rhizidiomycetaceae
Labyrinthulida;Labyrinthulidae
Labyrinthulida;Thraustochytriidae
Labyrinthulida;unclassified Labyrinthulida
Oomycetes;unclassified oomycetes
Pelagophyceae;Sarcinochrysidales
Pinguiophyceae;Pinguiochrysidales
Pirsonia;Other
Pseudopirsonia;Other
Synchromophyceae;Other
Synurophyceae;Synurales

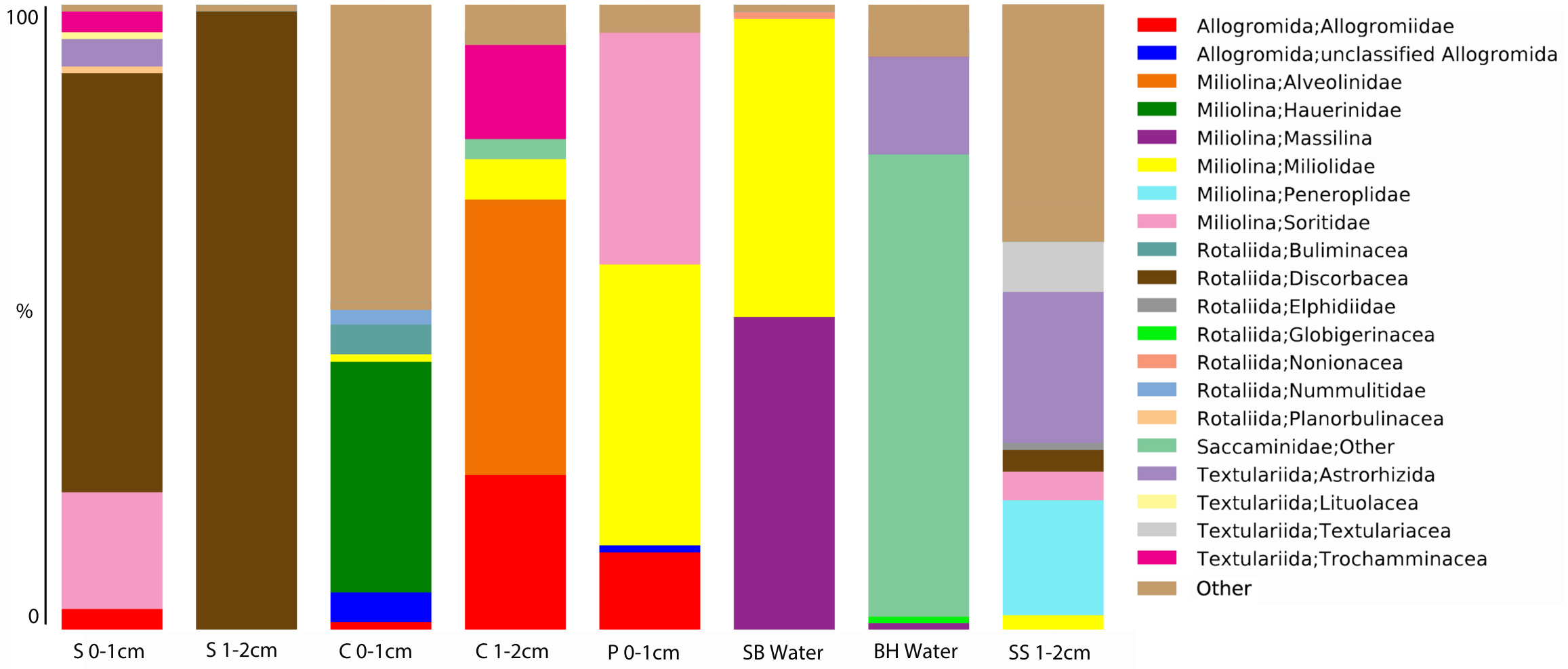
100
%
0
S 0-1cm
S 1-2cm
C 0-1cm
C 1-2cm
P 0-1cm
SB Water
BH Water
SS 1-2cm
Allogromida;Allogromiidae
Allogromida;unclassified Allogromida
Miliolina;Alveolinidae
Miliolina;Hauerinidae
Miliolina;Massilina
Miliolina;Miliolidae
Miliolina;Peneroplidae
Miliolina;Soritidae
Rotaliida;Buliminacea
Rotaliida;Discorbacea
Rotaliida;Elphidiidae
Rotaliida;Globigerinacea
Rotaliida;Nonionacea
Rotaliida;Nummulitidae
Rotaliida;Planorbulinacea
Saccaminidae;Other
Textulariida;Astrorhizida
Textulariida;Lituolacea
Textulariida;Textulariacea
Textulariida;Trochamminacea
Other

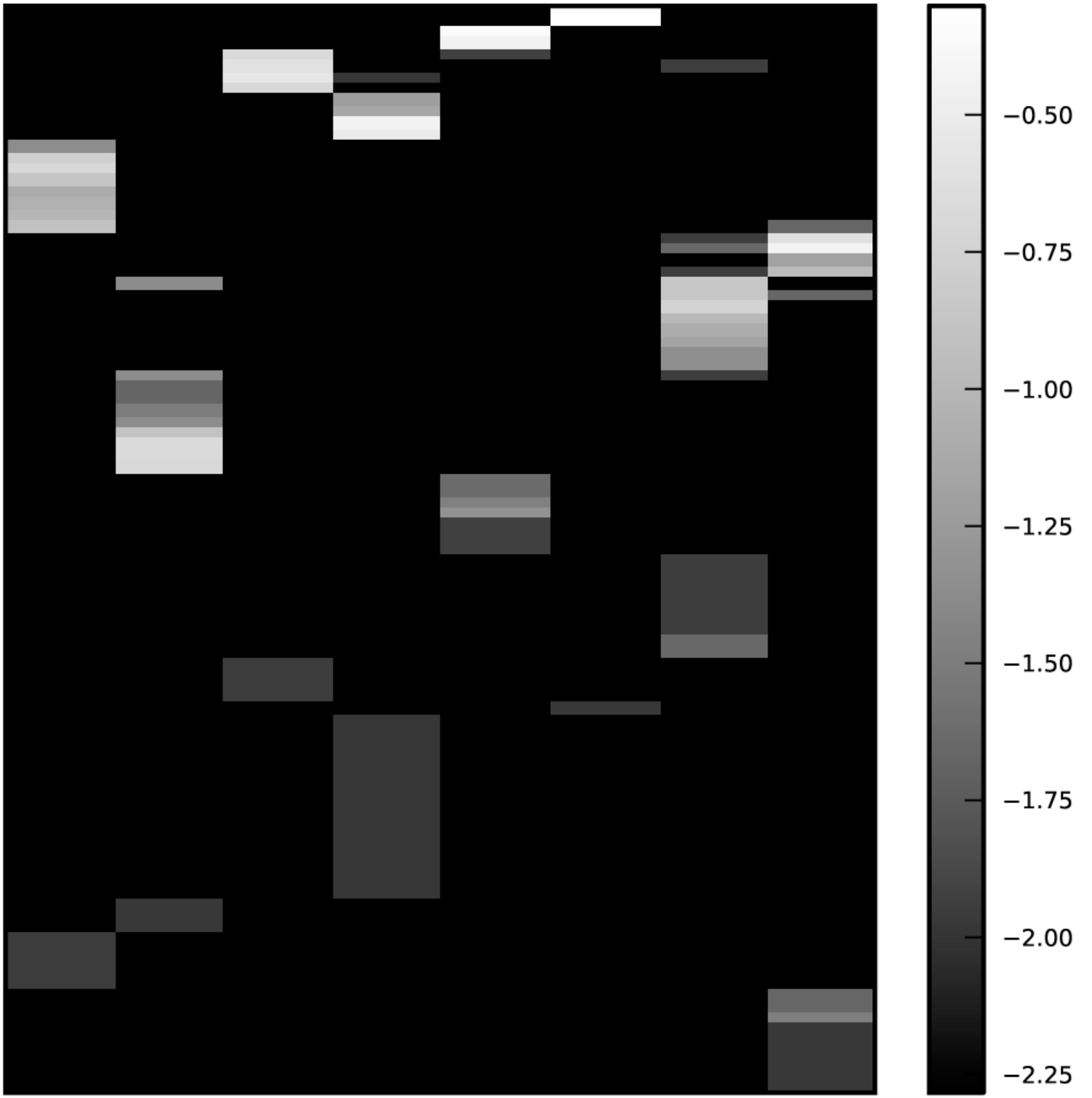
−0.50
−0.75
−1.00
−1.25
−1.50
−1.75
−2.00
−2.25
P
0-1cm
C
1-2cm
SB
water
BH
water
C
0-1cm
S
1-2cm
SS
1-2cm
S
0-1cm